

Modelling of shallow aquifers in interaction with overland water

Christophe Bourel^{a,*}, Catherine Choquet^b, Carole Rosier^a, Munkhgerel Tsegmid^a

^aUniv. Littoral Côte d'Opale, EA 2797 - LMPA, F- 62228 Calais, France

^bLa Rochelle Université, MIA, EA 3165, F-17031 La Rochelle, France

Abstract

In this work, we present a class of new efficient models for water flow in shallow unconfined aquifers, giving an alternative to the classical but less tractable 3D-Richards model. Its derivation is guided by two ambitions: any new model should be low cost in computational time and should still give relevant results at every time scale. We thus keep track of two types of flow occurring in such a context and which are dominant when the *ratio* thickness over longitudinal length is small: the first one is dominant in a small time scale and is described by a vertical 1D-Richards problem; the second one corresponds to a large time scale, when the evolution of the hydraulic head turns to become independent of the vertical variable. These two types of flow are appropriately modelled by, respectively, a one-dimensional and a two-dimensional system of PDEs boundary value problems. They are coupled along an artificial level below which the Dupuit hypothesis holds true (*i.e.* the vertical flow is instantaneous) in a way ensuring that the global model is mass conservative. Tuning the artificial level, which even can depend on an unknown of the problem, we browse the new class of models. We prove using asymptotic expansions that the 3D-Richards problem and each model of the class behaves the same at every considered time scale (short, intermediate and large) in thin aquifers. The results are illustrated by numerical simulations, showing especially that the new models results fit well with the ones obtained with the original 3d-Richards problem even in non-thin aquifers.

Keywords: Fluid flow modelling; Saturated and unsaturated porous media; Numerical simulations; Asymptotic analysis; Vertical Richards equations; Dupuit Hypothesis.

1. INTRODUCTION

Contamination of soil and groundwater is a major concern that affects all populated areas. Many works are thus developed for studying the vulnerability of aquifers with regard to agricultural, industrial, or sewage pollutions. There is an abundant literature on each of the involved processes (geological, physical, chemical...), so that we can consider that the corresponding model is already available. Nevertheless there is a so wide variety of processes (chemical, hydrogeological, anthropic) acting in a so wide range of temporal and geometrical length scales that the assembly of the corresponding model bricks, if considered like toolboxes of a software, is, at best, computationally expensive.

In this multi-scale context, a particularly interesting issue is a proper and tractable model for the exchanges between the overland and the underground waters. Indeed, the challenge consists in capturing very different physical phenomena, the fast and essentially vertical leakage coming from the surface through an unsaturated soil and the slow and essentially horizontal displacement in the saturated part of the aquifer, that are classically modelled by mathematical systems with very different structures. The question is all the more important that an accurate study of the interaction between the water table and the overland water is essential for many concerns, concerns that disallow the use of classical time upscaling processes. It is in particular crucial for studying the transport of chemical components in the aquifer. Indeed, it turns out that many chemical reactions occur in the

*Corresponding author: christophe.bourel@univ-littoral.fr

first meters of the subsoil, where oxygen is still very present. As a byproduct, the chemical species that reach the water table are not necessarily the same than those that have left the surface, and there is a large range of kinetics reaction times to handle with. There is actually no scale separation.

In the present paper, we focus on the hydrogeological question. We thus consider the displacement of a wetting phase (water) in the presence of a non-wetting fluid (air) in a porous medium. Assuming that the air present in the unsaturated zone has infinite mobility allows to use a model for immiscible fluid flow simplified by the Richards hypothesis. The saturation is thus considered as a monotone function depending of the pressure head and the so-called Richards model consists in a nonlinear three-dimensional equation of degenerate parabolic type. All the existing simplified models for the fluid displacement in aquifers are motivated by the characteristics of the flow in their saturated part. A form of stratification enables the definition of interfaces and the slowness of the natural dynamics ensures that these interfaces have a smooth and stable behaviour. Moreover the flows are essentially orthogonal to the walls (Dupuit's hypothesis). These points allow the vertical integration of the Richards equation in the saturated area and lead to the use of a family of 2D models developed since the 60's (see e.g. the works of Jacob Bear, [5, 6]). A main weakness of the approach by vertical integration lies in its justification. It is only valuable for very precise length and time scales, the time scale in particular being completely different of the typical durations of chemical reactions (see once again [5] for empirical and qualitative arguments, see [9] for asymptotic computations). However, such 2D models are widely used, even out of their validity range and even if it turns out to be especially difficult to properly couple them with the flow in the unsaturated part of the underground. Only numerical attempts were done in this direction. We mention [8] where the integrated model is directly coupled with a surface model (see also the references therein). The unsaturated area of the aquifer is taken into account in [12] using a 1D-Richards equation coupled with a simplified model in the saturated part. However, the study is purely numerical and the model is not mathematically justified. In [1], the latter kind of model is integrated into a computational code called "SHE" (for "European Hydrological System" and later became SHETRAN) in the case where the water table remains away from the ground level. See also [17], [10].

To the best of our knowledge, there is no mathematical justification for any "Dupuit-Richards" model specifying the hypotheses as well as the scales that allow its derivation from a more complete model (such as the 3D-Richards one).

Notice finally that the coupling of the surface and underground flows turns out to be more tractable when handling with a Richards equation (see e.g. [14] or [2] and [3] where the surface behavior is reduced to a Signorini boundary condition).

The goal of this work is to provide a simple model exploiting the low thickness of a confined or unconfined aquifer. In summary it consists in coupling purely vertical models (describing the flow at a small time scale) with a horizontal model (describing the flow at a long time scale). Clearly, given its construction, the model is simpler to manipulate numerically since the original 3D problem is replaced by the coupling of a 2D problem with several independent 1D-problems (which can be solved in parallel). Significant time savings are expected in the numerical processing.

This work could be viewed as another attempt using the numerically pragmatical methodology of [1] and leading to a "Dupuit-Richards" model. Yet, our approach is quite different. First, we actually derive a class of models, each of them being characterised by the definition of some virtual interface which does not necessarily coincide with the water table (especially when trying to optimize the error). It follows that a model of this class does not necessarily contains a Dupuit component. The position of the virtual interface may even be an unknown of our model. Next, we aim at describing the flow in a large range of time scales, and, more precisely without any assumption of scale separation. The idea consists in always capturing both the fast and slow components of the flow given by Richards 3D equations, whatever the time scale. Their coupling is done through flux terms ensuring that the model is mass conservative (and thus avoiding the criticism done in [15]). Finally, the large validity range of the new class of models is justified by an asymptotic study. But, as already mentioned, no time scale separation is assumed in the present paper so that we adopt a new methodology for the asymptotic arguments. Let $\varepsilon > 0$ describe the ratio of the aquifer's deepness over its characteristic horizontal length. Assume that ε is small. The usual approach would consist in choosing a reference time for the study, introducing an asymptotic expansion of the solution of the 3D-Richards system and using the scale separation for identifying the equations governing the main order terms of this ansatz. This is the classical process for deriving an effective model. Here the asymptotic

analysis is not used for deriving an effective model for a given reference time. Rather, it is used for proving that each model of our new class and the 3D-Richards equation are associated with the same effective problem for any time scale. Basically:

1. At short times, the horizontal flow is very small and the vertical one satisfies a 1D-Richards problem.
2. At non-short times, the vertical flow appears instantaneous. The corresponding pressure profile satisfies the stationary 1D-Richards problem. Then the hydraulic head H does not depend on the vertical variable z . This corresponds to the so-called Dupuit hypothesis.
3. At large times, the horizontal flux is non-zero. It is ruled by a 2D-horizontal diffusion equation where the conductivity is the vertical average of the permeability tensor on the *whole* depth of the aquifer.

The paper is organised as follows: In Section 2, we describe the geometry of the problem, the physical parameters and unknowns. The classical 3D-Richards model is recalled. The main result and numerical simulations are given in Section 3. Namely, we present the systems coupling the vertical and the horizontal flows and we comment on the model. Finally, the formal asymptotic analysis of our models and of the 3D-Richards model are performed and compared in Section 4.

2. DESCRIPTION OF THE PROBLEM

This section is devoted to the description of the domain of study, of the physical parameters and of the unknowns which are chosen for characterising the flow through the Richards model.

2.1. Geometry

The aquifer corresponds to a cylindrical domain $\Omega \subset \mathbb{R}^3$. For the sake of the simplicity, we assume vertical walls. The projection of Ω on any horizontal plane is an open domain $\Omega_x \subset \mathbb{R}^2$ with boundary $\partial\Omega_x$. The lower and upper bases of Ω are respectively the graphs of real-valued functions h_{bot} and h_{soil} such that

$$h_{\text{soil}}(x) > h_{\text{bot}}(x), \quad \forall x \in \Omega_x. \quad (2.1)$$

In summary the domain is given by:

$$\Omega = \{(x, z) \in \Omega_x \times \mathbb{R} \mid z \in]h_{\text{bot}}(x), h_{\text{soil}}(x)[\}. \quad (2.2)$$

We split the boundary $\partial\Omega$ of Ω in three parts (bottom, top and vertical)

$$\begin{aligned} \partial\Omega &= \Gamma_{\text{bot}} \sqcup \Gamma_{\text{soil}} \sqcup \Gamma_{\text{ver}}, \\ \Gamma_{\text{bot}} &:= \{(x, z) \in \Omega \mid z = h_{\text{bot}}(x)\}, \quad \Gamma_{\text{soil}} := \{(x, z) \in \Omega \mid z = h_{\text{soil}}(x)\}, \quad \Gamma_{\text{ver}} := \{(x, z) \in \Omega \mid x \in \partial\Omega_x\}. \end{aligned}$$

In the present paper, as already mentioned, we derive a class of models that are characterised by the position h of some virtual interface in the reservoir. For our construction, this function has to take its values in the semi-open interval $[h_{\text{bot}}, h_{\text{soil}})$. For numerical implementation, an easy recipe consists in replacing the condition $h < h_{\text{soil}}$ by $h \leq h_{\text{soil}} - \delta$ where δ is an arbitrary small positive real number. We thus introduce the auxiliary function h_{max} defined by

$$h_{\text{max}} = h_{\text{soil}} - \delta, \quad 0 < \delta \ll 1. \quad (2.3)$$

2.2. Three-dimensional Richards equation

We aim at deriving alternatives to the Richards equation. Let us briefly describe this classical model. In this paper we limit our study to a one-phase incompressible fluid which accordingly admits a constant density $\rho \in \mathbb{R}_+^*$. First, in multiphase systems, observations have shown that an increase of the saturation of the non-wetting phase leads to an increase of the capillary pressure. The Richards model is moreover based on the assumption that the air pressure in the underground equals the atmospheric pressure, thus is not an unknown of the problem. One thus assumes that the saturation and the relative conductivity of the soil are given as *functions* of the fluid pressure P ,

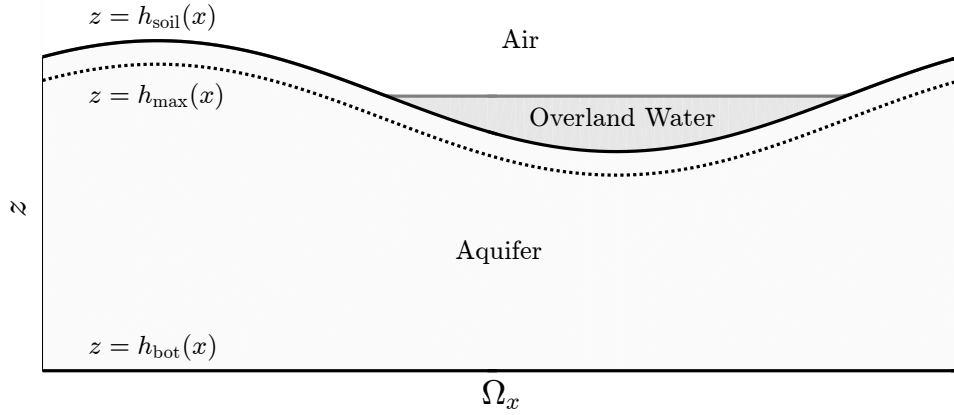


Figure 1: Bidimensional representation of the cylindrical geometry of the problem: $\Omega_x \subset \mathbb{R}$ is an interval.



Figure 2: Saturation and relative permeability in terms of the pressure: the Brooks and Corey model.

denoted respectively by $s = s(P)$ and $k_r = k_r(P)$. There is a large choice of available models for s and k_r . The most classical examples for an air-water system are the van Genuchten model [16], with no-explicit dependance on the bubbling pressure but with fitting parameters, and the Brooks and Corey model [4], that we use in the simulations below:

$$s(P) = \begin{cases} (P_s/P)^\lambda & \text{if } P < P_s \\ 1 & \text{if } P \geq P_s \end{cases}, \quad k_r(P) = \begin{cases} (P_s/P)^\gamma & \text{if } P < P_s \\ 1 & \text{if } P \geq P_s \end{cases}, \quad (2.4)$$

where $\lambda > 0$, $\gamma = 2 + 3\lambda$ and $P_s < 0$. Notice that our model would easily adapt to hysteretic soil properties ([11], [13]). Since these methods, as of today, do not permit three-dimensional calculations, we guess that our 1D-2D models are even more interesting for their implementation than the 3D-Richards model. The important point is that these models are such that

$$s(P) = 1 \iff P \geq P_s \quad \text{and} \quad k_r(P) = 1 \iff P \geq P_s. \quad (2.5)$$

In particular, the water pressure is greater than the bubbling pressure P_s if and only if the soil is completely saturated (P_s being a fixed real number). The graphs of the functions s and k_r given by the Brooks-Corey model used below for the numerical simulations are represented in Figure 2 (the parameters are given at the beginning of Subsection 3.4).

The soil transmission properties are characterised by the porosity function, $\phi = \phi(x, z) \in (0, 1)$, and the permeability tensor, $K_0(x, z)$. The latter is a 3×3 symmetric positive definite tensor which describes the conductivity of the *saturated* soil at the position $(x, z) \in \Omega$. We introduce $K_{xx} \in \mathcal{M}_{22}(\mathbb{R})$, $K_{zz} \in \mathbb{R}^*$ and $K_{xz} \in \mathcal{M}_{21}(\mathbb{R})$ such that

$$K_0 = \begin{pmatrix} K_{xx} & K_{xz} \\ K_{xz}^T & K_{zz} \end{pmatrix}. \quad (2.6)$$

The fluid is characterised by its pressure P and its velocity v solving the following Richards problem:

$$\begin{cases} \phi \frac{\partial s(P)}{\partial t} + \operatorname{div}(v) = 0 & \text{in }]0, T[\times \Omega \\ v = -k_r(P) K_0 \left(\frac{1}{\rho g} \nabla P + e_3 \right) & \text{in }]0, T[\times \Omega \\ \alpha P + \beta v \cdot n = F & \text{on }]0, T[\times \Gamma_{\text{soil}} \\ v \cdot n = 0 & \text{on }]0, T[\times (\Gamma_{\text{bot}} \cup \Gamma_{\text{ver}}) \end{cases} \quad (2.7)$$

where g is the gravity constant and e_3 is the unitary vertical vector pointing up. The first equation describes the mass conservation of the constant density fluid in the case of an incompressible soil. The second equation is the Darcy's law associated with the nonlinear anisotropic conductivity $k_r(P) K_0$. The boundary condition $v \cdot n = 0$ on Γ_{bot} corresponds to the impermeable layer at the bottom of the aquifer. The same is assumed on Γ_{ver} to simplify the presentation. The condition at the soil level Γ_{soil} is a Robin condition associated with given $(\alpha, \beta) \in (\mathbb{R}_+)^2 \setminus \{0, 0\}$ and $F: \Gamma_{\text{soil}} \rightarrow \mathbb{R}$.

Remark 1 (Dominant behaviors in a shallow aquifer). In Section 4 we investigate the behavior of the flow described by the 3D-Richards equations in the case of a thin aquifer and for various time scales. Let us summarise the conclusions of this asymptotic analysis. They might shed light on the comments about our models in the next section.

1. At any time scale, the dominant flow is the one in the vertical direction (see for example (4.9) in which the horizontal diffusion term appears multiplied by the small parameter ε).
2. In the short time scale ($T \sim 1$), the horizontal flow is very small and the vertical one solves a classical 1D-Richards problem.
3. In non-short time scales ($T \sim \varepsilon^{-1}$ or $T \sim \varepsilon^{-2}$), the vertical flow appears as being instantaneous. The corresponding pressure profile satisfies a stationary 1D-Richards problem. Then the pressure is $P = \rho g(H - z)$ where the hydraulic head H does not depend on the vertical variable z . The velocity is horizontal. This corresponds to the so-called Dupuit hypothesis.
4. In the long time scale ($T \sim \varepsilon^{-2}$), the horizontal flow is non-zero and it is ruled by a 2D-horizontal diffusion equation where the conductivity is the vertical average of the permeability tensor on the *whole* depth of the aquifer, from h_{bot} to h_{soil} .

3. MAIN RESULT AND NUMERICAL SIMULATIONS

3.1. Models coupling vertical 1d-Richards flow and Dupuit horizontal flow

Each of our models splits the description of the flow into two subregions of Ω (possibly time-dependent). These zones are defined by a function $h = h(t, x)$ such that $h_{\text{bot}} \leq h < h_{\text{soil}}$:

$$\Omega_h^-(t) := \{(x, z) \in \Omega \mid z < h(x, t)\} \quad \text{and} \quad \Omega_h^+(t) := \{(x, z) \in \Omega \mid z > h(x, t)\}, \quad (3.1)$$

$$\Gamma_h := \{(x, z) \in \Omega \mid z = h(x, t)\}. \quad (3.2)$$

We emphasise that choosing the level h corresponds to the specification of one of the models of our class. The function h can even be an unknown of our problem, more precisely depending of an unknown of the problem (see condition (3.8) below).

On the other hand we introduce the following tensor M_0 which will act as an effective permeability tensor:

$$M_0 = \begin{pmatrix} S_0 & 0 \\ 0 & 0 \end{pmatrix}, \quad S_0 = K_{xx} - \frac{1}{K_{zz}} K_{xz} K_{zx}. \quad (3.3)$$

The 2×2 matrix S_0 is the Schur complement of the block K_{zz} in the tensor K_0 . Since K_0 is a symmetric positive definite matrix (see just before (2.6)), the same holds for S_0 . We then introduce the averaged conductivity tensor \tilde{K} defined in $]0, T[\times \Omega_x$ for any function $\tilde{H} = \tilde{H}(t, x)$ by

$$\tilde{K}(\tilde{H})(t, x) = \int_{h_{\text{bot}}(x)}^{h_{\text{soil}}(x)} k_r(\rho g(\tilde{H}(t, x) - z)) M_0(x, z) dz. \quad (3.4)$$

Finally, for the 2D part of the model, we introduce the notations $\nabla_x = (\partial_{x_1}, \partial_{x_2}, 0)^T$ for the horizontal gradient and $\text{div}_x(v) = \nabla_x \cdot v = \partial_{x_1} v_1 + \partial_{x_2} v_2$ for the horizontal divergence of $v \in \mathbb{R}^3$.

The model. Our coupled model consists in finding the pressure P , the velocity v and the auxiliary unknowns u , w , \tilde{H} and h such that:

- In $\Omega_h^+(t)$ the following 1D-Richards equation holds

$$\begin{cases} \phi \frac{\partial s(P)}{\partial t} + \frac{\partial}{\partial z}(u \cdot e_3) = 0 & \text{for } t \in]0, T[, \quad (x, z) \in \Omega_h^+(t) \\ \alpha P + \beta u \cdot e_3 = F & \text{for } (t, x) \in]0, T[\times \Gamma_{\text{soil}} \\ P(t, x, h(t, x)) = \rho g (\tilde{H}(t, x) - h(t, x)) & \text{for } (t, x) \in]0, T[\times \Omega_x \\ P(0, x, z) = P_{\text{init}}(x, z) & \text{for } (x, z) \in \Omega_h^+(0) \end{cases} \quad (3.5)$$

- In $\Omega_h^-(t)$ the pressure P satisfies

$$P(t, x, z) = \rho g (\tilde{H}(t, x) - z) \quad \text{for } t \in [0, T[, \quad (x, z) \in \Omega_h^-(t) \quad (3.6)$$

- The hydraulic head solves in Ω_x

$$\begin{cases} \text{div}_x \left(\tilde{K}(\tilde{H}) \nabla_x \tilde{H} \right) = (u \cdot e_3)|_{\Gamma_h^+} & \text{for } (t, x) \in]0, T[\times \Omega_x \\ \tilde{K}(\tilde{H}) \nabla_x \tilde{H} \cdot n = 0 & \text{for } (t, x) \in]0, T[\times \partial\Omega_x \\ \tilde{H}(0, x) = H_{\text{init}}(x) & \text{for } x \in \Omega_x \end{cases} \quad (3.7)$$

where $(u \cdot e_3)|_{\Gamma_h^+}$ denotes the trace of $u \cdot e_3$ on Γ_h from above.

- The level $z = h$ below which we consider the vertical flow to be instantaneous is set such that

$$h_{\text{bot}}(x) \leq h(t, x) \leq \max \left\{ \min \left\{ \tilde{H}(t, x) - \frac{P_s}{\rho g}, h_{\text{max}}(x) \right\}, h_{\text{bot}}(x) \right\}, \quad (t, x) \in [0, T[\times \Omega_x. \quad (3.8)$$

- The velocity v is defined in Ω by

$$\begin{cases} v = u + w & \text{for } t \in]0, T[, \quad (x, z) \in \Omega \\ u = -k_r(P) \left(\frac{1}{\rho g} \frac{\partial P}{\partial z} + 1 \right) K_0 e_3 & \text{for } t \in]0, T[, \quad (x, z) \in \Omega \\ w = -k_r(\rho g (\tilde{H} - z)) M_0 \nabla_x \tilde{H} & \text{for } t \in]0, T[, \quad (x, z) \in \Omega \end{cases} \quad (3.9)$$

The coupled model (3.5)–(3.9) depends on the definition of the function h . Although all intermediate choices respecting (3.8) are allowed, we will focus in the next on the two extremal choices

$$h(t, x) = h_{\text{bot}}(x), \quad (3.10)$$

$$h(t, x) = \max \left\{ \min \left\{ \tilde{H}(t, x) - \frac{P_s}{\rho g}, h_{\text{max}}(x) \right\}, h_{\text{bot}}(x) \right\} := h_s(t, x), \quad (3.11)$$

and on the intermediate one

$$h(t, x) = \max \left\{ \min \left\{ \tilde{H}(t, x) - \frac{P_s + R}{\rho g}, h_{\text{max}}(x) \right\}, h_{\text{bot}}(x) \right\}, \quad (3.12)$$

where R is some positive function possibly depending on \tilde{H} .

The class of models (3.5)–(3.9) is an alternative to the 3D-Richards problem for describing the flow in a shallow aquifer in a large range of time scales. This model is designed to fulfill the two following properties:

- to be simpler to handle numerically than the 3D-Richards model
- to behave like the 3D-Richards model for any time scale when the *ratio* ε of the deepness over the horizontal length of the aquifer is small¹. For example the behaviors presented in Remark 1 are respected.

The first property holds for (3.5)–(3.9) since the 3D original Richards problem is replaced by the coupling of a 2D-problem with a lot of independent 1D-problems which can be solved in parallel. Significant time savings are expected in the computations. The second property is justified in Section 4. The idea is to study the limit $\varepsilon \rightarrow 0$ of the solution of the 3D-Richards equations and to derive formally the associated effective problem. The same asymptotic analysis is performed for the coupled models (3.5)–(3.9) and shows that the corresponding effective problems are exactly the same for every considered time scale and for every choice of h satisfying (3.8).

Remark 2. It is natural to think that it is possibly not so useful to couple two phenomena which does not hold at the same time scale, since by essence they can not interact with each other. But the notion of time *scale* is senseless for a fixed physical situation and we just employ this term to enlighten the interpretations. The notion of scale has a precise sense when a sequence of problems is considered, for example parametrised by a small parameter ε tending to zero with the reference time of study depending on ε . This is what we do in Section 4 where ε is the *ratio* deepness/length of the aquifer. This limit process shows that the two kinds of flow appear at different time scales and then do not interact with each other. Nevertheless, the coupled problem (3.5)–(3.9) is *not* an effective problem and holds without time scale separation assumption. The *depth / width* ratio of the aquifer is then a fixed positive number given by the geometry of the aquifer. In particular, "short" and "long" time scales flows can interact without either being negligible or instantaneous.

The remainder of this subsection is devoted to comments on the new models (3.5)–(3.9). Before splitting those comments according to the choice of the function h , we prove that the model is always mass conservative.

Mass conservation. Let $M_{\text{tot}}(t)$ the total mass of the water contained in domain Ω at time t . We denote by M_h^+ (resp. M_h^-) the mass of the water filling the domain Ω_h^+ (resp. Ω_h^-). We have

$$M_h^+(t) = \rho \int_{\Omega_x} \int_{h(t,x)}^{h_{\text{soil}}} \phi s(P) dz dx, \quad M_h^-(t) = \rho \int_{\Omega_x} \int_{h_{\text{bot}}(x)}^{h(t,x)} \phi dz dx, \quad (3.13)$$

$$M_{\text{tot}}(t) = M_h^+(t) + M_h^-(t). \quad (3.14)$$

Proposition 3.1. *The total mass satisfies for all $t \in (0, T)$:*

$$\frac{\partial}{\partial t} M_{\text{tot}} = -\rho \int_{\Omega_x} (u \cdot e_3)|_{\Gamma_{\text{soil}}} dx.$$

PROOF. By using relation (3.13) and (3.14) it comes

$$\frac{\partial}{\partial t} M_{\text{tot}} = \rho \int_{\Omega_x} \int_{h_{\text{bot}}(x)}^{h(t,x)} \phi \frac{\partial s(P)}{\partial t} dz dx + \rho \int_{\Omega_x} \int_{h(t,x)}^{h_{\text{soil}}(x)} \phi \frac{\partial s(P)}{\partial t} dz dx = \rho \int_{\Omega_x} \int_{h(t,x)}^{h_{\text{soil}}(x)} \phi \frac{\partial s(P)}{\partial t} dz dx, \quad (3.15)$$

where the first equality is due to $s(P) = 1$ in $]h_{\text{bot}}(x), h(t,x)[$ (indeed $P \geq P_s$ by (3.6) and (3.8)). Thanks to the first equation in (3.5) we deduce

$$\int_{\Omega_x} \int_{h(t,x)}^{h_{\text{soil}}(x)} \phi \frac{\partial s(P)}{\partial t} dz dx = \int_{\Omega_x} (u \cdot e_3)|_{\Gamma_h^+} dx - \int_{\Omega_x} (u \cdot e_3)|_{\Gamma_{\text{soil}}} dx. \quad (3.16)$$

Finally by (3.7) and after an integration by parts

$$\int_{\Omega_x} (u \cdot e_3)|_{\Gamma_h^+} dx = \int_{\partial\Omega_x} \tilde{K}(\tilde{H}) \nabla_x \tilde{H} \cdot n = 0. \quad (3.17)$$

The result is obtained by plugging (3.16) and (3.17) in (3.15). \square

¹however the numerical simulations below show good results even for a *ratio* of order 0.1, which is not exceeded by the large majority of the unconfined aquifers.

3.2. Comments on the model in the case (3.10)

In this case, we have $h = h_{\text{bot}}$, then $\Omega_h^+ = \Omega$, $\Omega_h^- = \emptyset$ and $\Gamma_h = \Gamma_{\text{bot}}$ (see (3.1)). The coupled model (3.5)–(3.9) reduces in: finding the pressure P , the velocity v and the auxiliary unknowns u , w and \tilde{H} such that:

$$\begin{cases} v = u + w & \text{for } t \in]0, T[, \quad (x, z) \in \Omega \\ u = -k_r(P) \left(\frac{1}{\rho g} \frac{\partial P}{\partial z} + 1 \right) K_0 e_3 & \text{for } t \in]0, T[, \quad (x, z) \in \Omega \\ w = -k_r(\rho g(\tilde{H} - z)) M_0 \nabla_x \tilde{H} & \text{for } t \in]0, T[, \quad (x, z) \in \Omega \end{cases} \quad (3.18)$$

$$\begin{cases} \phi \frac{\partial s(P)}{\partial t} + \frac{\partial}{\partial z} (u \cdot e_3) = 0 & \text{for } t \in]0, T[, \quad (x, z) \in \Omega \\ \alpha P + \beta u \cdot e_3 = F & \text{for } (t, x, z) \in]0, T[\times \Gamma_{\text{soil}} \\ P = \rho g(\tilde{H} - h_{\text{bot}}) & \text{for } (t, x, z) \in]0, T[\times \Gamma_{\text{bot}} \\ P(0, x, z) = P_{\text{init}}(x, z) & \text{for } (x, z) \in \Omega \end{cases} \quad (3.19)$$

$$\begin{cases} -\text{div}_x (\tilde{K}(\tilde{H}) \nabla_x \tilde{H}) = -(u \cdot e_3)|_{\Gamma_{\text{bot}}} & \text{for } (t, x) \in]0, T[\times \Omega_x \\ \tilde{K}(\tilde{H}) \nabla_x \tilde{H} \cdot n = 0 & \text{for } (t, x) \in]0, T[\times \partial \Omega_x \\ \tilde{H}(0, x) = H_{\text{init}}(x) & \text{for } x \in \Omega_x \end{cases} \quad (3.20)$$

This setting corresponds to the simplest form of the model (3.5)–(3.9) since (3.20) is a classical boundary value problem. Nevertheless the simulations below illustrate that it is not the better form of approximation for the 3D-Richards equation.

Velocity of the flow. The velocity v of the flow turns out to be the superposition of the two velocities u and w which respectively describe the fast and slow components of the flow. Actually u (resp. w) is the dominant component of the flow in the short time scale (resp. large time scale).

Fast component of the flow: globally vertical. The unknown u represents the velocity associated with the pressure P by the one dimensional Darcy's law given in the second equation of (3.18). This one is deduced from the 3D law (see the second equation of (2.7)) by neglecting the horizontal components of the gradient of the pressure P . By construction the field u is vertical if the conductivity tensor K_0 introduced in (2.6) is such that $K_{xz} = 0$ but it may admit a non-zero horizontal component in the anisotropic case.

Furthermore the mass conservation equation (3.19) holds. The pressure P then satisfies the following vertical Richards equation where the horizontal variable $x \in \Omega_x$ appears only as a parameter:

$$\phi \frac{\partial s(P)}{\partial t} - \frac{\partial}{\partial z} \left(k_r(P) K_{zz} \left(\frac{1}{\rho g} \frac{\partial P}{\partial z} + 1 \right) \right) = 0 \quad \text{in }]0, T[\times \Omega. \quad (3.21)$$

The original 3D-Richards problem reduces to the latter equation when the horizontal diffusion terms are neglected. In the short-time scale indeed, those turn to be non-dominant in shallow aquifers as announced in Remark 1 and shown in Section 4.

The boundary condition on Γ_{soil} remains the same than in the 3D-Richards problem. But on the bottom Γ_{bot} , the structure of the boundary condition changes and becomes of Dirichlet type, namely $P(t, x, h_{\text{bot}}(t, x)) = \rho g(\tilde{H}(t, x) - h_{\text{bot}}(t, x))$. In fact, even if this Dirichlet condition holds, we do not allow the water flowing out the aquifer through the bottom boundary. Indeed the possibly non-zero flux $(u \cdot e_3)|_{\Gamma_{\text{bot}}}$ appears as a source term in the first equation of (3.20), so that, as proved in Proposition 3.14, the coupled model is globally mass-conservative. The particular value $P = \rho g(\tilde{H} - h_{\text{bot}})$ for the bottom Dirichlet condition, has been chosen so that the fast and slow flows are correctly coupled. This point is further explained in the next paragraph.

Slow component of the flow: globally horizontal. On the one hand, introduce the auxiliary pressure Q ,

$$Q := \rho g(\tilde{H} - z),$$

for which \tilde{H} plays the role of the hydraulic head. Since \tilde{H} does not depend on z , we have $(\rho g)^{-1} \partial_z Q + 1 = 0$. The first consequence is that the unknown w satisfies (see (3.18))

$$w = -k_r(Q) M_0 \nabla_x \tilde{H}.$$

We recover here the velocity associated to Q by the classical Darcy's law for the conductivity $k_r(Q) M_0$. The second consequence is that Q is ruled by

$$\frac{\partial}{\partial z} \left(k_r(Q) K_{zz} \left(\frac{1}{\rho g} \frac{\partial Q}{\partial z} + 1 \right) \right) = 0 \quad \text{in }]0, T[\times \Omega,$$

that is the stationary version of equation (3.21).

On the other hand, we expect P to solve the same stationary problem when the duration of the experiment and when the boundary conditions allow the 1D-Richards problem (3.21) to reach its stationary state. Notice that such a vertical affine profile is also expected in the 3D-Richards model in any non-short time scale (see Remark 1 and Section 4). When this situation occurs, the hydraulic head $H := P/\rho g + z$ is constant with respect to z . The Dirichlet boundary condition on h_{bot} in (3.19) then implies that

$$H(t, x, z) = H(t, x, h_{\text{bot}}(x)) = \frac{P(t, x, h_{\text{bot}}(x))}{\rho g} + h_{\text{bot}}(x) = \tilde{H}(t, x).$$

Accordingly, in any non-short time scale, we get $H \approx \tilde{H}$ and then $P \approx Q$ in Ω . This is the reason of the particular choice $P = \rho g(\tilde{H} - h_{\text{bot}})$ for the Dirichlet boundary condition on h_{bot} in (3.19). Roughly speaking, the couple (Q, w) characterizes the flow in a long-time experiment in which the vertical flow seems instantaneous with respect to the horizontal one.

Unlike the velocity u , the field w is horizontal both in the isotropic and anisotropic cases due to the definition of the tensor M_0 . The computations leading to the definition of M_0 are done in Section 4. Let us give here some qualitative arguments. For large times, w is the main order term of the flow which turns out to be horizontal. The velocity w is also related to some hydraulic head, say L , by the classical Darcy's law $w = -k_r K_0 \nabla L$ (as in the Richards equation (2.7); see (4.45)). But since w is horizontal we have

$$0 = w \cdot e_3 = -k_r K_0 \nabla L \cdot e_3 = -k_r K_{zx} \nabla_x L - k_r K_{zz} \frac{\partial L}{\partial z} \quad \text{and then} \quad \frac{\partial L}{\partial z} = -k_r \frac{K_{zx}}{K_{zz}} \nabla_x L$$

if $K_{zz} \neq 0$ as assumed in this paper, otherwise the question is trivial. Accordingly, in the expression of $w = -k_r K_0 \nabla L$, only the term $\nabla_x L$ appears and it follows $w = -k_r M_0 \nabla_x L$. Notice that the tensor M_0 reduces to K_{xx} in the isotropic case $K_{xz} = K_{zx} = 0$.

Moreover w depends on z only through the term $k_r(\rho g(\tilde{H} - z)) M_0$ which decreases to 0 when z increases above $\tilde{H} - P_s/\rho g$. This decrease is fast in general depending on the soil characteristic function k_r . Then, roughly speaking, the horizontal component of the flow is maximum in the saturated part and almost vanishing in the unsaturated one far from the capillary fringe.

The evolution of the "stationary pressure" Q is ruled by the first equation of (3.20). This is an horizontal mass-conservation equation associated with the average velocity $\tilde{w} := -\tilde{K}(\tilde{H}) \nabla_x \tilde{H} = \int_{h_{\text{bot}}}^{h_{\text{soil}}} w \, dz$. The right-hand side is the source term computed from the 1D-Richards problem and which transfers the mass from the vertical description to the horizontal one.

Notice that in this model (3.18)-(3.20), the Dupuit hypothesis is not considered. We precise this point in the next Subsection.

3.3. Comments on the model in the cases (3.11) and (3.12)

Now we come back to the model (3.5)–(3.9) in which we set the virtual interface h by

$$h(t, x) = \max \left\{ \min \left\{ \tilde{H}(t, x) - \frac{P_s + R}{\rho g}, h_{\max}(x) \right\}, h_{\text{bot}}(x) \right\}, \quad (3.22)$$

for a given non-negative function R possibly depending on \tilde{H} . In the numerical simulations at the end of this section, we consider the constant cases $R = 0$, corresponding to (3.11), and $R = 3$. Choosing (3.11) could be guessed as the most intuitive choice since it means in general splitting the domain along the water table, thus separating the flows in the saturated and in the unsaturated areas. But simulations show that it is not necessary the optimal choice for the quality of the 3D-Richards approximation.

Velocity of the flow. As previously, the velocity v of the flow results from the contribution of a fast component u and of a slow one w . The set Ω_h^- is no more empty in general and an additional brick is introduced in the model for describing the flow in this area. We start by giving some properties of the interface Γ_h .

Interface discriminating the flow behaviors. As seen in (3.1), the sets $\Omega_h^-(t)$ and $\Omega_h^+(t)$ are characterised by h . In view of the constraint (3.8), the condition

$$h_{\text{bot}}(x) \leq h(t, x) \leq h_{\max}(x) \quad (3.23)$$

holds for all $(t, x) \in]0, T[\times \Omega_x$. Due to (3.6) and (3.8) the pressure at the level $z = h(t, x)$ satisfies for all $(t, x) \in]0, T[\times \Omega_x$:

$$P(t, x, h(t, x)) \begin{cases} = P_s + R & \text{if } h_{\text{bot}}(x) < h(t, x) < h_{\max}(x), \\ \geq P_s + R & \text{if } h(t, x) = h_{\max}(x), \\ \leq P_s + R & \text{if } h(t, x) = h_{\text{bot}}(x). \end{cases} \quad (3.24)$$

In particular, thanks to (2.5) and since $R \geq 0$ we get

$$s(P(t, x, z)) = 1 \quad \text{if } h_{\text{bot}}(x) < z \leq h(t, x), \quad (3.25)$$

which means that the set $\Omega_h^-(t)$ contains a saturated part of the aquifer for any choice of $R \geq 0$. More precisely, the soil is fully saturated in $\Omega_h^-(t)$ for every $t \in]0, T[$ if $R > 0$, and if $R = 0$, that is for (3.11), Ω_h^- can be interpreted as the water table (see Remark 3 below for precisions).

By construction $h(t, x) \leq h_{\max}$ so that the interval $]h(t, x), h_{\text{soil}}(x)[$ remains non-empty for all $(t, x) \in]0, T[\times \Omega_x$. Then we do not have to explicit a direct coupling of the flow in Ω_h^- with the one in the overland. The coupling between Ω_h^- and Ω_h^+ is sufficient.

Fast component of the flow: globally vertical, a part being instantaneous. We start by remarking that, as in the previous case, the velocity u is related to P by the vertical Darcy's law (3.9). Moreover the same 1D-Richards equation (3.5) holds, but now, only in the upper part of the aquifer. In particular, in the short-time scale, the dominant vertical flow in $\Omega_h^+(t)$ remains well described.

The main difference between cases $h = h_{\text{bot}}$ and $h \neq h_{\text{bot}}$ is related to the vertical flow in the saturated area $\Omega_h^-(t)$. Indeed, the pressure profile (3.6) now holds in Ω_h^- and in particular u is zero in Ω_h^- . As said before, this affine profile is expected in the non-short time scale when the vertical flow appears instantaneous. Hence, the model (3.5)–(3.9) describes precisely the vertical flow in Ω_h^+ and assumes that this flow is instantaneous in Ω_h^- . Such an assumption is classical in models of saturated shallow aquifers and is known as the Dupuit hypothesis. Then, the model (3.5)–(3.9) in the cases (3.12) can be seen as the coupling of a Dupuit horizontal flow in a saturated part at the bottom of the aquifer with many vertical 1D-Richards flows for a precise description of the leaking fluxes from the overland to the water table.

Notice that, even if $h \neq h_{\text{bot}}$, the model (3.5)–(3.9) does approximate the 3D-Richards problem at every time scale when the ration $\varepsilon = \text{deepness}/\text{horizontal length}$ tends to zero. Indeed, Proposition 4.1 below holds for any choice of function h such that (3.8) is satisfied. This is explained by the following points in short times:

- From the 3D-Richards problem, we expect a vertical description given by the 1D-Richards in the whole Ω , with a vanishing flux at the bottom of the domain (see (4.21)).
- From our model, we get 1D-Richards only in Ω_h^+ with a zero flux in Ω_h^- (see proof of the short-time scale near equation (4.57)) and the continuity of the pressure.

In fact, these problems are exactly the same.

The field u is non-singular thanks to the continuity condition satisfied by P on Γ_h (see (3.5) and (3.6)). As for $h = h_{\text{bot}}$, the particular value of the Dirichlet condition on Γ_h has been chosen for a proper coupling of the fast and slow components of the flow. This is further developed in the next paragraph. However if $u \cdot e_3$ has a trace on the boundary Γ_h of Ω_h^+ , this one is non-zero in general whereas $u \cdot e_3 = 0$ in Ω_h^- . This is a notable difference with the case $h = h_{\text{bot}}$.

Slow component of the flow. Again, we introduce the auxiliary pressure $Q = \rho g(\tilde{H} - z)$ and we remark that now $P = Q$ in $\Omega_h^-(t)$ (even for short times). The fact that $P \approx Q$ in the whole Ω for any non-short times comes, as in the case $h = h_{\text{bot}}$, from the Dirichlet condition $P = \rho g(\tilde{H} - z)$ which holds on Γ_h .

The evolution of (Q, w) is characterized by the evolution of \tilde{H} given in (3.7). In this case where $\Omega_h^-(t)$ is non-empty in general, we can explicit a little more the dynamic of \tilde{H} . This is detailed in the next paragraph.

Evolution of the hydraulic head. Rewrite the problem (3.7) using the first equation of (3.5) averaged on $[h, h_{\text{soil}}]$:

$$-\operatorname{div}_x \left(\tilde{K}(\tilde{H}) \nabla_x \tilde{H} \right) = -u|_{\Gamma_{\text{soil}}} \cdot e_3 - \int_{h(t,x)}^{h_{\text{soil}}(x)} \phi \frac{\partial s(P)}{\partial t} dz \quad \text{in }]0, T[\times \Omega_x. \quad (3.26)$$

Since $s(P) = 1$ for $z \in [h_{\text{bot}}, h]$, we get

$$-\operatorname{div}_x \left(\tilde{K}(\tilde{H}) \nabla_x \tilde{H} \right) = -u|_{\Gamma_{\text{soil}}} \cdot e_3 - \frac{\partial}{\partial t} \int_{h_{\text{bot}}(x)}^{h_{\text{soil}}(x)} \phi s(P) dz \quad \text{in }]0, T[\times \Omega_x, \quad (3.27)$$

or equivalently by using the Leibniz rule in (3.26) and $s(P)|_{z=h} = 1$:

$$\phi|_{\Gamma_h} \frac{\partial h}{\partial t} - \operatorname{div}_x \left(\tilde{K}(\tilde{H}) \nabla_x \tilde{H} \right) = -u|_{\Gamma_{\text{soil}}} \cdot e_3 - \frac{\partial}{\partial t} \left(\int_{h(t,x)}^{h_{\text{soil}}(x)} \phi s(P) dz \right) \quad \text{in }]0, T[\times \Omega_x. \quad (3.28)$$

The hydraulic head \tilde{H} is characterized by the latter equation completed by the limit conditions in (3.8). This problem is a non-linear degenerate diffusion equation. Indeed, the diffusion tensor $\tilde{K}(\tilde{H})$ vanishes when \tilde{H} tends to $-\infty$. If moreover (3.11) holds, in view of (3.8), the time derivative can be expressed as

$$\frac{\partial h}{\partial t} = C(\tilde{H}) \frac{\partial \tilde{H}}{\partial t} \quad \text{with} \quad C(\tilde{H}) = \begin{cases} 1 & \text{if } \tilde{H} - P_s / \rho g \in]h_{\text{bot}}, h_{\text{max}}[\\ 0 & \text{if not.} \end{cases}$$

The right-hand side of the first equation in (3.7) plays the role of a *source term* and represents for each $x \in \Omega$ the evolution of the amount of water which flows in or out the column $]h(t, x), h_{\text{soil}}(x)[$ through its lower boundary $h(t, x)$. As we have shown in Proposition 3.1 above, this source term ensures the mass conservation in the coupled model (3.5)–(3.9). Of course this term also depends (non linearly) on the solution \tilde{H} . However this dependence is more easy to handle than the one given in the first equation of (3.7). In particular, the expression (3.28) is well adapted to the numerical implementation of the coupled problem (3.5)–(3.9).

Notice that the level $z = h_s$, defined in (3.11), represents the interface between the saturated and unsaturated part of the aquifer according to the auxiliary pressure $Q := \rho g(\tilde{H}(t, x) - z)$. In particular $Q(t, x, h_s(t, x)) = P_s$ if $h_s(t, x) \in (h_{\text{bot}}(x), h_{\text{soil}}(x))$ (regardless of the choice of $R \geq 0$ in (3.22)). The conductivity tensor $\tilde{K}(\tilde{H})$ defined in (3.4) can be then decomposed into two parts:

$$\tilde{K}(\tilde{H})(t, x) = \tilde{C}_0 + \int_{h_s(t,x)}^{h_{\text{soil}}(x)} k_r(Q) M_0(x, z) dz \quad (3.29)$$

where \tilde{C}_0 is the averaged conductivity of the saturated soil, *i.e.*

$$\tilde{C}_0 = \int_{h_{\text{bot}}(x)}^{h_s(t,x)} M_0(x, z) dz.$$

In classical models for the saturated part of an aquifer obtained by vertical integration under the Dupuit's assumption, the definition of the effective conductivity (see for example [6]) reduces to \tilde{C}_0 instead of $\tilde{K}(\tilde{H})$, the latter being a little greater. The quantity \tilde{C}_0 takes into account the horizontal flow in the saturated part but it ignores the (little) one in the unsaturated part, in particular close to the interface $z = h_s$ where the capillary effects lead to a non-negligible saturation. In practice, the smaller h_s , the more significant is the difference $\tilde{K}(\tilde{H}) - \tilde{C}_0$. In particular, if a part of the bottom of the aquifer is not saturated, that is $h_s = h_{\text{bot}}$, considering only the vanishing conductivity \tilde{C}_0 whereas $\tilde{K}(\tilde{H})$ remains positive is physically incorrect.

3.4. Numerical simulations

In this section we compare numerically the original 3D-Richards model (2.7) and the coupled model (3.5)–(3.9) for several choices of h satisfying (3.8).

Physical parameters and geometry. All the simulations are done with the following set of data. Denoting I_3 the 3×3 identity matrix we set:

$$s(P) = (P_s/P)^\lambda, \quad k_r(P) = (P_s/P)^{2+3\lambda}, \quad (P_s, \lambda) = (-1.5, 3), \quad \rho = 1, \quad \phi = 0.1, \quad K_0 = 0.1 I_3.$$

To lighten the numerical results, we consider the simplified 2D aquifer $\Omega =]-5, 0[\times \Omega_x$, $\Omega_x =]0, L_x[$. In the experiments illustrated in Figures 3 and 4, the horizontal length is $L_x = 28$. In those of Figure 5, $L_x \in [21, 393]$. The parameter δ in (2.3) is chosen as small as possible, that is equal to the size of one vertical mesh. We assume an impermeable layer at the bottom and the top of the aquifer.

Visualisation. For the visualization of the results, we introduce a function h_{sat} representing in a lot of cases the top level of the saturated region at the bottom of the aquifer (*i.e.* the water table). Let $h_{\text{sat}} = h_{\text{sat}}(t, x)$ and the set $\Omega_{h_{\text{sat}}}^-(t)$ be defined for a given pressure $P = P(t, x, z)$ by

$$h_{\text{sat}}(t, x) := \sup I_{t,x}, \quad I_{t,x} := \{z \in [h_{\text{bot}}(x), h_{\text{max}}(x)] \mid P(t, x, z') > P_s, \forall z' \in [h_{\text{bot}}(x), z]\}, \quad (3.30)$$

$$\Omega_{h_{\text{sat}}}^-(t) := \{(x, z) \in \Omega \mid z < h_{\text{sat}}(t, x)\}. \quad (3.31)$$

By construction and if P is continuous we have

$$P(t, x, h_{\text{sat}}(t, x)) \begin{cases} = P_s & \text{if } h_{\text{bot}} < h_{\text{sat}} < h_{\text{max}} \\ \geq P_s & \text{if } h_{\text{sat}} = h_{\text{max}} \\ \leq P_s & \text{if } h_{\text{sat}} = h_{\text{bot}} \end{cases}$$

and $P(t, x, z) \geq P_s$ for all $z \in]h_{\text{bot}}, h_{\text{sat}}[$. In particular the soil is fully saturated in $\Omega_{h_{\text{sat}}}^-(t)$ for every $t \in]0, T[$.

Remark 3. Notice that the set $\Omega_{h_{\text{sat}}}^-$ does not coincide with *the* saturated region of the soil at the bottom of the aquifer. Indeed a saturated region just over $z = h_{\text{sat}}$ is possible for example if $P \geq P_s$ also in $\Omega \setminus \Omega_{h_{\text{sat}}}^-$. The interface $z = h_{\text{sat}}$ then describes

- either the interface between the saturated part at the bottom of the aquifer and the unsaturated part above in the simplest setting,
- or a level between two saturated part when for example a saturated front flow down and reach $\Omega_{h_{\text{sat}}}^-$,
- or the bottom of the aquifer when $h_{\text{sat}} = h_{\text{bot}}$, that is when there is no saturated part at the bottom,
- or the maximum allowed height $h_{\text{sat}} = h_{\text{max}}$ when, roughly speaking, the water table overflows.

Of course here, since $h_{\text{sat}}(t, x) \leq h_{\text{soil}} - \delta$ by (2.3), the set $\Omega_{h_{\text{sat}}}^-$ cannot reach the soil level h_{soil} . In this sense $\Omega_{h_{\text{sat}}}^-$ does not represent the physical water table which possibly touches the soil level. We only have done this choice for the definition of h_{sat} to recover the unknown h in the maximal case (3.11) and thus to facilitate the visualisation.

Numerical scheme. For the numerical approximation of the problem (3.5)–(3.9) we use mass-conservative fully implicit time schemes associated with finite elements methods in space for both horizontal and vertical directions. The schemes for (3.10) and (3.12) differ:

- In the case (3.10), we solve directly equation (3.7) in which the right-hand side $(u \cdot e_3)|_{\Gamma_h^+}$ is seen as a Dirichlet to Neumann operator depending on \tilde{H} and obtained by solving the 1D-vertical Richards equations. This non-linear term is treated with a Newton method.
- In the case (3.12), the nonlinear coupling between the 1D-vertical Richards equations and the 1D-horizontal diffusion equation is performed by using a Picard's fixed-point method at each time step. This one alternatively solves (3.5) (for an explicit \tilde{H} and h) and (3.28) (for an explicit right-hand side).

In any case all the 1D-Richards equations remain independent at the discrete level and can be solved in parallel.

Reference flowing experiment. At time $t = 0$, we consider a setting where the function h_{sat} introduced in (3.30) corresponds to the height of the water table. To show the influence of the deepness of the saturated area, we choose a function $h_{\text{sat}}(0, \cdot)$ which goes smoothly from -4.5 on the left part of the aquifer to -2.5 on the right one:

$$h_{\text{sat}}(0, x) = \begin{cases} -4.5 + 2 e^{-\left(\frac{15}{L_x}\right)^2 (x-0.55L_x)^2} & \text{in } [0, 0.55L_x], \\ -2.5 & \text{in }]0.55L_x, L_x]. \end{cases}$$

The initial pressure P is defined by $P(0, x, z) = \rho g (h_{\text{sat}}(0, x) - z) + P_s$ for all (x, z) except near two rectangular regions above $z = h_{\text{sat}}$ where the pressure goes smoothly to the saturation value P_s , corresponding to an infiltration process. These rectangles are

$$R_1 =]L_x/10, 3L_x/10[\times]-3.5, -1.7[\quad \text{and} \quad R_2 =]7L_x/10, 9L_x/10[\times]-2, -0.2[. \quad (3.32)$$

This initial situation is drawn in the first picture of Figure 3. In every picture the gray scale corresponds to the saturation value, the maximal darkness corresponding to $s \approx 1$.

The total time of the experiment is 4 days. The solution of the classical Richards problem at time 0, 10, 20 and 96 hours respectively, is drawn in Figure 3. The graph of the visualization function h_{sat} defined in (3.30) is also plotted. Its evolution will be used for comparing the original Richards model with the coupled model (3.5)–(3.9).

At time $t = 10$ the water initially in rectangles R_1 and R_2 started to flow down. In the right part, some water coming from R_2 have reached the saturated water table inducing an increase of its level. In the mean time, we see in the middle of the domain Ω_x that the water moves to the left and that the function h_{sat} is smoother than the initial one.

At time $t = 20$ the water initially in rectangle R_1 has continued to flow down and is about to reach the water table. It is important to notice that this flow was essentially along the vertical direction. In particular the water front which is very close to h_{sat} is approximately horizontal as in the initial situation.

After some time almost all the water initially located in the rectangle supplies have reached the water table. Then the interface h_{sat} becomes flat and is associated with a pressure admitting the stationary profile $P(t, x, z) = P_s + \rho g (h_{\text{sat}}(t, x) - z)$.

Comparison of the models. In this part we compare the solution of the classical Richards model with the one obtained by using the coupled model (3.5)–(3.9). We test three particular choices for the function h satisfying (3.8): the minimal one (3.10), the maximal one (3.11) and an intermediate one given by (3.12) for $R = 3$. All data remain the same as in the previous paragraph. In this paper, we focus on the evolution of the functions h_{sat} defined by (3.30). As indicated in Remark 3, this function roughly represents the upper level of the water table. In the following we denote by h_{sat}^{2d} the level coming from the reference 2d-Richards model and we denote by h_{sat}^a , h_{sat}^b and h_{sat}^c the ones coming from the model (3.5)–(3.9) with the function h given respectively by (3.10), (3.11) and (3.12).

The functions h_{sat}^{2d} , h_{sat}^a , h_{sat}^b and h_{sat}^c are plotted in Figure 4 at time $t \in \{10, 24, 48, 96\}$ (in hours). We of course do not plot the initial situation which is the same for each model and is the one of the reference test case described in the previous paragraph. The curve h_{sat}^{2d} is the reference one and is plotted with a black solid line in Figure 4.

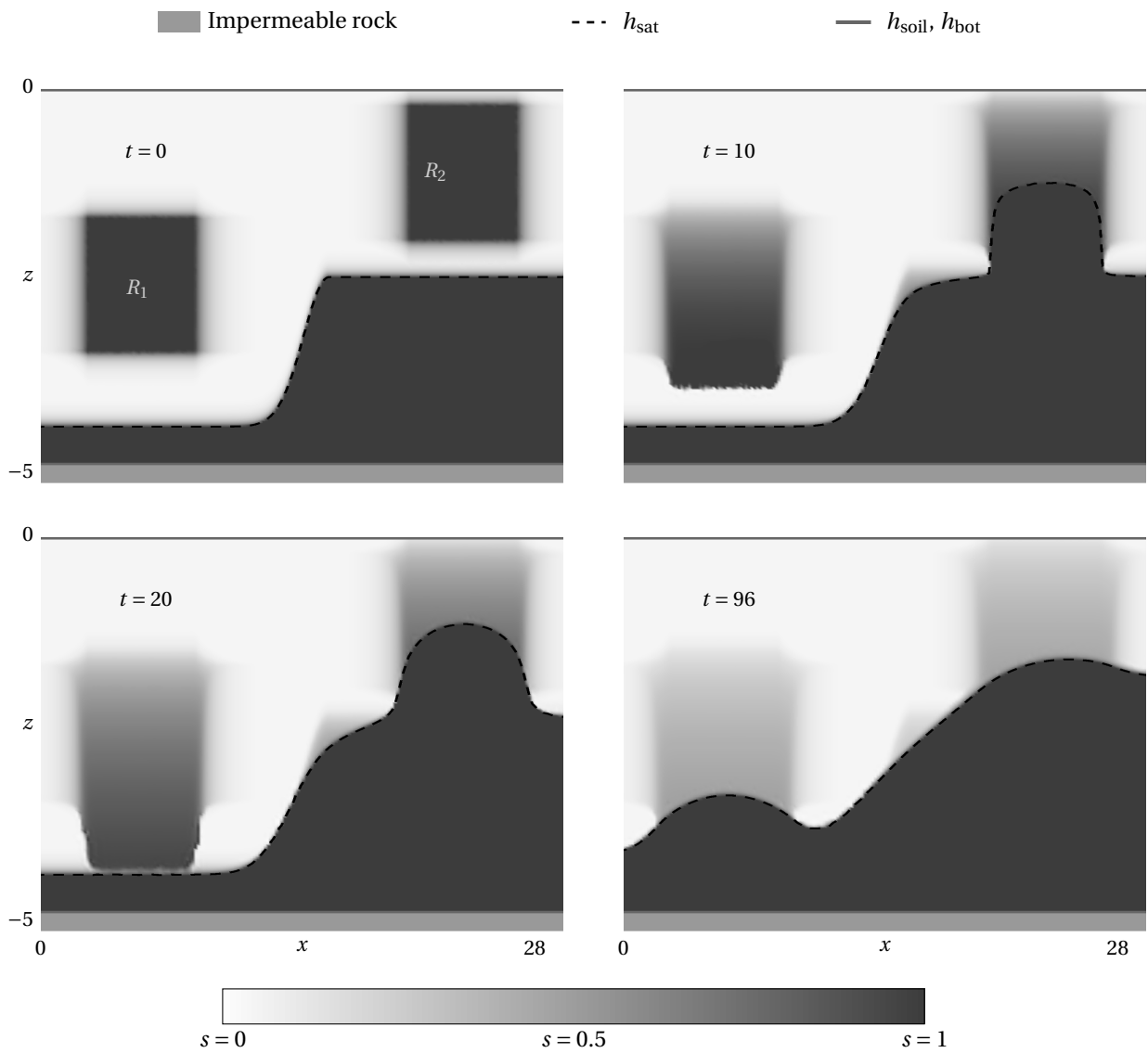


Figure 3: Solution of the classical Richards problem in the reference test case.

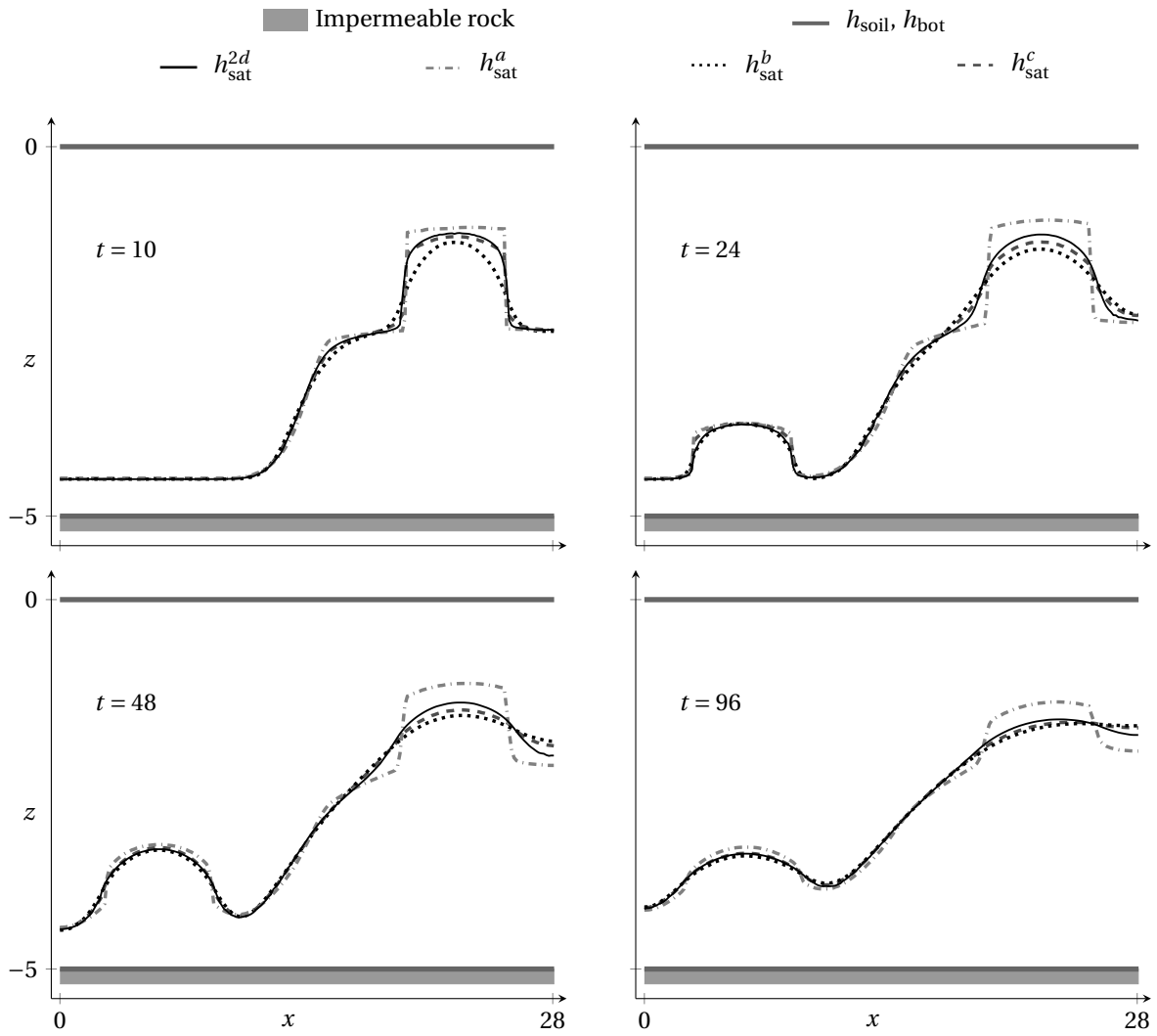


Figure 4: Evolution of the iso-pressure $P = P_s$ obtained from the classical Richards equation (h_{sat}^{2d}) and from the coupled model for three choices of h given by (3.10), (3.11) and (3.12) (h_{sat}^{κ} for $\kappa \in \{a, b, c\}$ respectively). The test case is the one of Figure 3.

Bear in mind that the function h characterizes the level below which the vertical flow is assumed to be instantaneous (instead of being described by the 1D-Richards equation). In every case, the horizontal flow is ruled by equation (3.7).

- In the case (3.10), $h = h_{\text{bot}}$. The vertical flow is described by the 1D-Richards model in the whole domain, even in the saturated part below the level $z = h_{\text{sat}}^a$. The horizontal flow in this case seems to be slower than the one given by the Richards model (compare the gray dot-dashed line with the black solid one in Figure 4).
Roughly the idea is that in this case the water have to travel along the whole vertical direction before reaching the level $z = h = h_{\text{bot}}$. Then the flux $(u \cdot e_3)|_{\Gamma_{\text{bot}}}$ at the bottom of the aquifer takes a lot of time to increase when the water coming from rectangles R_1 and R_2 reaches the water table. This flux being the source term in equation (3.7), the function \tilde{H} increases with some delay and the corresponding horizontal flow is slower.
- In the case (3.11), $h = h_{\text{sat}}^b$. This case is opposite of the previous one in the sense that the vertical flow in the whole saturated zone $\Omega_{h_{\text{sat}}}^-$ is considered to be instantaneous. Then, when the water coming from rectangles R_1 and R_2 reaches the water table, the flux $(u \cdot e_3)|_{\Gamma_h}$ increases very quickly. So does the corresponding hydraulic head \tilde{H} and the horizontal flow is very and even too fast (see the black dotted line compared to the black solid line in Figure 4).
- In the case (3.12) for $R = 3$, $h_{\text{bot}} \leq h \leq h_{\text{sat}}^c$. The corresponding flow should exhibit an intermediate behavior between the two previous ones. Here, the value $R = 3$ was chosen so that h_{sat}^c is very close to the reference one h_{sat}^{2d} (see the gray dashed line).

Notice that in every situation, the error between h_{sat}^{2d} and h_{sat}^κ , $\kappa \in \{a, b, c\}$, is smaller in the left part of the domain than in the right one. This is due to the fact that the saturated zone is thinner in this region. For a very thin saturated region, considering an instantaneous vertical flow or the one given by the vertical 1D-Richards problem gives similar results. Conversely, the thicker the saturated water table is, the more the results issued from the two extremal situations (3.10) and (3.11) differ from the reference one. Basically, h_{sat}^b is expected to move too fast while h_{sat}^a moves too slowly. In this kind of deep situation and if the *ratio* between the deepness and the length of the aquifer is not so small, one of the intermediate choices (3.12) is obviously more appropriate.

Error made by the coupled model versus the ratio deepness/largeness. In the previous simulations, where $\Omega =]0, 28[\times] - 5, 0[$, the *ratio* $\varepsilon = \text{deepness}/\text{length}$ of the aquifer is such that $1/\varepsilon = 5.6$. It is important to notice that even in this case of large ratio ε the error between the original Richards model and the coupled model (3.5)–(3.9) in the case (3.12) is particularly small (see the dashed plot in Figure 4). This supports the fact that the coupled model may be considered for approaching the Richards model also in an aquifer which is not so shallow. This guess is confirmed by the results plotted in Figure 5. The evolution of the error $\|h_{\text{sat}}^{2d} - h_{\text{sat}}^\kappa\|_{L^1(]0, T[\times\Omega_x)}$ for $\kappa \in \{a, b, c\}$ is drawn in terms of the ratio $1/\varepsilon$.

As expected all the errors decrease with ε . Moreover, the intermediate case (3.12) is always the best, mainly in the case of a “large” value of ε . After comes the maximal choice. The worst choice is the maximal one (3.10) but with an error which decreases a lot with ε .

Remark 4. The accuracy of the model depends on the choice of R in (3.22), e.g. for minimizing the error $\|h_{\text{sat}}^{2d} - h_{\text{sat}}^\kappa\|_{L^p(]0, T[\times\Omega_x)}$. This optimization process is postponed to a forthcoming work.

4. FORMAL ASYMPTOTIC EXPANSION

In this section, the 3D-Richards problem (2.7) and the coupled model (3.5)–(3.9) are compared using asymptotic analysis arguments. We prove that these models behave the same, whatever the time scale, when the *ratio* between the characteristic deepness and the length of the shallow aquifer tends to zero.

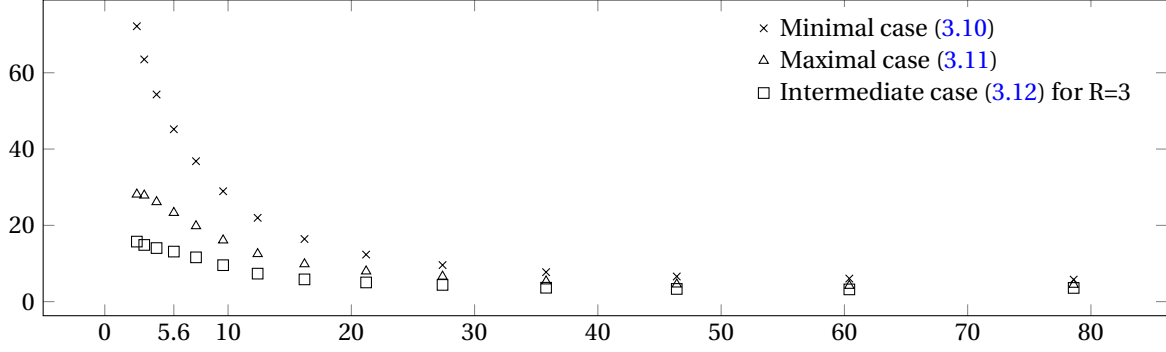


Figure 5: Cumulative error in space and time $\|h_{\text{sat}}^{2d} - h_{\text{sat}}^{\kappa}\|_{L^1([0, T] \times \Omega)}$ versus the ratio length/deepness $= 1/\varepsilon$ of the aquifer ($\kappa \in \{a, b, c\}$). Function h_{sat}^{2d} is the iso-pressure $P = P_s$ in the original 2d-Richards problem and h_{sat}^{κ} is the one associated with the coupled problems for three different choices of h satisfying (3.8). The test case is the one of figure 3.

4.1. Dimensionless form of the 3D-Richards and coupled problems

Introduce a fixed dimensionless reference domain $\bar{\Omega}$ of type (2.2) and a dimensionless real number $\bar{T} > 0$. Fix $\bar{\Omega}_x$, \bar{h}_{soil} and \bar{h}_{bot} such that

$$\bar{\Omega} = \left\{ (\bar{x}, \bar{z}) \in \bar{\Omega}_x \times \mathbb{R} \mid \bar{z} \in]\bar{h}_{\text{bot}}(\bar{x}), \bar{h}_{\text{soil}}(\bar{x})[\right\}.$$

To obtain a rescaled version of equations (2.7) and (3.5)–(3.9) in the domain $]0, \bar{T}[\times \bar{\Omega}$, we introduce positive reference numbers L_x, L_z, T . Then, keeping the same notations as in Section 3, we have:

- The physical variables are given by

$$x = L_x \bar{x}, \quad z = L_z \bar{z}, \quad t = \frac{T}{\bar{T}} \bar{t}.$$

- The corresponding physical domain Ω is given as in (2.2) with

$$\Omega_x = L_x \bar{\Omega}_x, \quad h_{\text{soil}}(x) = L_z \bar{h}_{\text{soil}}(\bar{x}), \quad h_{\text{bot}}(x) = L_z \bar{h}_{\text{bot}}(\bar{x}).$$

- The unknowns are such that

$$\begin{aligned} \bar{P}(\bar{t}, \bar{x}, \bar{z}) &= P(t, x, z), & \bar{v}(\bar{t}, \bar{x}, \bar{z}) &= v(t, x, z), & \bar{u}(\bar{t}, \bar{x}, \bar{z}) &= u(t, x, z), & \bar{w}(\bar{t}, \bar{x}, \bar{z}) &= w(t, x, z), \\ L_z \bar{H}(\bar{t}, \bar{x}) &= \tilde{H}(t, x), & L_z \bar{h}(\bar{t}, \bar{x}) &= h(t, x). \end{aligned}$$

- The reference subdomains are

$$\Omega_h^-(\bar{t}) = \{(\bar{x}, \bar{z}) \in \bar{\Omega}_x \times \mathbb{R} \mid \bar{z} \in]\bar{h}_{\text{bot}}(\bar{x}), \bar{h}(\bar{t}, \bar{x})[\}, \quad \Omega_h^+(\bar{t}) = \{(\bar{x}, \bar{z}) \in \bar{\Omega}_x \times \mathbb{R} \mid \bar{z} \in]\bar{h}(\bar{t}, \bar{x}), \bar{h}_{\text{soil}}(\bar{x})[\}.$$

- The reference boundaries are $\bar{\Gamma}_{\text{bot}} := \{(\bar{x}, \bar{z}) \in \bar{\Omega} \mid \bar{z} = \bar{h}_{\text{bot}}(\bar{x})\}$, $\bar{\Gamma}_{\text{soil}} := \{(\bar{x}, \bar{z}) \in \bar{\Omega} \mid \bar{z} = \bar{h}_{\text{soil}}(\bar{x})\}$ and $\bar{\Gamma}_{\text{ver}} := \{(\bar{x}, \bar{z}) \in \bar{\Omega} \mid \bar{x} \in \partial \bar{\Omega}_x\}$.

- The reference exterior normals are

$$\bar{n}(\bar{x}, \bar{z}) = \begin{cases} \left(e_3 - \frac{L_z}{L_x} \nabla_{\bar{x}} \bar{h}_{\text{soil}}(\bar{x}) \right) \left(\frac{L_z^2}{L_x^2} |\nabla_{\bar{x}} \bar{h}_{\text{soil}}(\bar{x})|^2 + 1 \right)^{-1/2} & \text{on } \bar{\Gamma}_{\text{soil}} \\ \left(\frac{L_z}{L_x} \nabla_{\bar{x}} \bar{h}_{\text{bot}}(\bar{x}) - e_3 \right) \left(\frac{L_z^2}{L_x^2} |\nabla_{\bar{x}} \bar{h}_{\text{bot}}(\bar{x})|^2 + 1 \right)^{-1/2} & \text{on } \bar{\Gamma}_{\text{bot}} \\ n(x, z) & \text{on } \bar{\Gamma}_{\text{ver}} \end{cases}$$

where the vector \bar{n} is horizontal and does not change during the rescaling.

- The saturation and relative conductivity satisfy

$$s(\bar{P}) = s(P), \quad k_r(\bar{P}) = k_r(P). \quad (4.1)$$

It means that the reference saturation and relative permeability are of order one. Indeed P and \bar{P} take the same values, independently of the scale change.

- For the conductivities, we set

$$\bar{K}_0(\bar{x}, \bar{z}) = K_0(x, z), \quad \bar{M}_0(\bar{x}, \bar{z}) = M_0(x, z), \quad (4.2)$$

$$\bar{K}(\bar{H})(\bar{t}, \bar{x}) = L_z \int_{\bar{h}_{\text{bot}}(\bar{x})}^{\bar{h}_{\text{soil}}(\bar{x})} k_r(\rho g(\bar{H}(\bar{t}, \bar{x}) - \bar{z})) \bar{M}_0 d\bar{z}. \quad (4.3)$$

We choose (4.2) for the sake of simplicity in the presentation. Indeed, we could also introduce K and M such that $K\bar{K}_0(\bar{x}, \bar{z}) = K_0(x, z)$ and $M\bar{M}_0(\bar{x}, \bar{z}) = M_0(x, z)$ and then perform the same study assuming that $K/L_x = \mathcal{O}(\varepsilon)$, $M/L_x = \mathcal{O}(\varepsilon)$ and $K/L_z = \mathcal{O}(1)$.

- The source term is

$$\bar{F}(\bar{t}, \bar{x}) = F(t, x)$$

Dimensionless Richards problem. Introducing the latter quantities in (2.7), we get the following set of rescaled equations:

$$\frac{\bar{T}}{T} \phi \frac{\partial s(\bar{P})}{\partial \bar{t}} + \frac{1}{L_x} \text{div}_{\bar{x}}(\bar{v}) + \frac{1}{L_z} \frac{\partial \bar{v}}{\partial \bar{z}} = 0 \quad \text{in }]0, \bar{T}[\times \bar{\Omega}, \quad (4.4)$$

$$\bar{v} = -k_r(\bar{P}) \bar{K}_0 \left(\frac{1}{L_x} \frac{1}{\rho g} \nabla_{\bar{x}} \bar{P} + \left(\frac{1}{L_z} \frac{1}{\rho g} \frac{\partial \bar{P}}{\partial \bar{z}} + 1 \right) e_3 \right) \quad \text{in }]0, \bar{T}[\times \bar{\Omega}, \quad (4.5)$$

$$\bar{v} \cdot \left(\frac{L_z}{L_x} \nabla_{\bar{x}} \bar{h}_{\text{bot}} - e_3 \right) = 0 \quad \text{on }]0, \bar{T}[\times \bar{\Gamma}_{\text{bot}}, \quad (4.6)$$

$$\alpha \bar{P} \left(\frac{L_z^2}{L_x^2} \|\nabla_{\bar{x}} \bar{h}_{\text{soil}}\|^2 + 1 \right)^{1/2} + \beta \bar{v} \cdot \left(e_3 - \frac{L_z}{L_x} \nabla_{\bar{x}} \bar{h}_{\text{soil}} \right) = \bar{F} \left(\frac{L_z^2}{L_x^2} \|\nabla_{\bar{x}} \bar{h}_{\text{soil}}\|^2 + 1 \right)^{1/2} \quad \text{on }]0, \bar{T}[\times \bar{\Gamma}_{\text{soil}}, \quad (4.7)$$

$$\bar{v} \cdot \bar{n} = 0 \quad \text{on }]0, \bar{T}[\times \bar{\Gamma}_{\text{ver}}. \quad (4.8)$$

Since the aquifer is assumed to be very thin with respect to its horizontal width, the quantity L_z/L_x is very small. We choose to consider an aquifer with a fixed height of order $L_z = 1$ and a large horizontal dimension $L_x = 1/\varepsilon$ for $\varepsilon \ll 1$. We get

- the mass conservation equation which depends on the time scaling choice T :

$$\frac{\bar{T}}{T} \phi \frac{\partial s(\bar{P})}{\partial \bar{t}} + \varepsilon \text{div}_{\bar{x}}(\bar{v}) + \frac{\partial \bar{v} \cdot e_3}{\partial \bar{z}} = 0 \quad \text{in }]0, \bar{T}[\times \bar{\Omega} \quad (4.9)$$

- associated with the following Darcy's law and boundary conditions:

$$\begin{cases} \bar{v} = -k_r(\bar{P}) \bar{K}_0 \left(\frac{\varepsilon}{\rho g} \nabla_{\bar{x}} \bar{P} + \left(\frac{1}{\rho g} \frac{\partial \bar{P}}{\partial \bar{z}} + 1 \right) e_3 \right) & \text{in }]0, \bar{T}[\times \bar{\Omega} \\ \alpha \bar{P} \left(\varepsilon^2 \|\nabla_{\bar{x}} \bar{h}_{\text{soil}}\|^2 + 1 \right)^{1/2} + \beta \bar{v} \cdot \left(e_3 - \varepsilon \nabla_{\bar{x}} \bar{h}_{\text{soil}} \right) = \left(\varepsilon^2 \|\nabla_{\bar{x}} \bar{h}_{\text{soil}}\|^2 + 1 \right)^{1/2} \bar{F} & \text{on }]0, \bar{T}[\times \bar{\Gamma}_{\text{soil}} \\ \bar{v} \cdot \bar{n} = 0 & \text{on }]0, \bar{T}[\times \bar{\Gamma}_{\text{ver}} \\ \bar{v} \cdot \left(\varepsilon \nabla_{\bar{x}} \bar{h}_{\text{bot}} - e_3 \right) = 0 & \text{on }]0, \bar{T}[\times \bar{\Gamma}_{\text{bot}} \end{cases} \quad (4.10)$$

Dimensionless coupled Dupuit-Richards model. By introducing the same parameter $\varepsilon \ll 1$, the rescaled coupled problem (3.5)–(3.9) reads:

- The velocity problem:

$$\begin{cases} \bar{v} = \bar{u} + \bar{w} & \text{for } \bar{t} \in]0, \bar{T}[, \quad (\bar{x}, \bar{z}) \in \bar{\Omega} \\ \bar{u} = -k_r(\bar{P}) \left(\frac{1}{\rho g} \frac{\partial \bar{P}}{\partial \bar{z}} + 1 \right) \bar{K}_0 e_3 & \text{for } \bar{t} \in]0, \bar{T}[, \quad (\bar{x}, \bar{z}) \in \bar{\Omega} \\ \bar{w} = -\varepsilon k_r(\rho g(\bar{H} - \bar{z})) \bar{M}_0 \nabla_{\bar{x}} \bar{H} & \text{for } \bar{t} \in]0, \bar{T}[, \quad (\bar{x}, \bar{z}) \in \bar{\Omega} \end{cases} \quad (4.11)$$

- The 1D-Richards equation in the transition zone:

$$\begin{cases} \phi \frac{\bar{T}}{\bar{T}} \frac{\partial s(\bar{P})}{\partial \bar{t}} + \frac{\partial}{\partial \bar{z}} (\bar{u} \cdot e_3) = 0 & \text{for } \bar{t} \in]0, \bar{T}[, \quad (\bar{x}, \bar{z}) \in \Omega_h^+(\bar{t}) \\ \alpha \bar{P} + \beta \bar{u} \cdot e_3 = \bar{F} & \text{for } (\bar{t}, \bar{x}) \in]0, \bar{T}[\times \bar{\Gamma}_{\text{soil}} \\ \bar{P}(\bar{t}, \bar{x}, \bar{h}(\bar{t}, \bar{x})) = \rho g (\bar{H}(\bar{t}, \bar{x}) - \bar{h}(\bar{t}, \bar{x})) & \text{for } (\bar{t}, \bar{x}) \in]0, \bar{T}[\times \bar{\Omega}_x \\ \bar{P}(0, \bar{x}, \bar{z}) = \bar{P}_{\text{init}}(\bar{x}, \bar{z}) & \text{for } (\bar{x}, \bar{z}) \in \Omega_h^+(0) \end{cases} \quad (4.12)$$

- The pressure problem in the water table:

$$\bar{P}(\bar{t}, \bar{x}, \bar{z}) = \rho g (\bar{H}(\bar{t}, \bar{x}) - \bar{z}) \quad \text{for } \bar{t} \in]0, \bar{T}[, \quad (\bar{x}, \bar{z}) \in \Omega_h^-(\bar{t}) \quad (4.13)$$

- The hydraulic head problem:

$$\begin{cases} \varepsilon^2 \operatorname{div}_{\bar{x}} (\bar{K}(\bar{H}) \nabla_{\bar{x}} \bar{H}) = \bar{u}|_{\Gamma_h^+} \cdot e_3 & \text{for } (\bar{t}, \bar{x}) \in]0, \bar{T}[\times \bar{\Omega}_x \\ \bar{K}(\bar{H}) \nabla_{\bar{x}} \bar{H} \cdot \bar{n} = 0 & \text{for } (\bar{t}, \bar{x}) \in]0, \bar{T}[\times \partial \bar{\Omega}_x \\ \bar{H}(0, \bar{x}) = \bar{H}_{\text{init}}(\bar{x}) & \text{for } \bar{x} \in \bar{\Omega}_x \end{cases} \quad (4.14)$$

Equivalently, by using (3.27), the first equation of (4.14) admits the formulation: for $(\bar{t}, \bar{x}) \in]0, \bar{T}[\times \bar{\Omega}_x$

$$\varepsilon^2 \operatorname{div}_{\bar{x}} (\bar{K}(\bar{H}) \nabla_{\bar{x}} \bar{H}) = \bar{u}|_{\bar{\Gamma}_{\text{soil}}} \cdot e_3 + \frac{\bar{T}}{T} \frac{\partial}{\partial \bar{t}} \left(\int_{\bar{h}_{\text{bot}}(\bar{x})}^{\bar{h}_{\text{soil}}(\bar{x})} \phi s(\bar{P}) d\bar{z} \right) \quad (4.15)$$

- The definition of the interface separating the two different kind of flows:

$$\bar{h}_{\text{bot}}(\bar{x}) \leq \bar{h}(\bar{t}, \bar{x}) \leq \max \left\{ \min \left\{ \bar{H}(\bar{t}, \bar{x}) - \frac{P_s}{\rho g}, \bar{h}_{\text{max}}(\bar{x}) \right\}, \bar{h}_{\text{bot}}(\bar{x}) \right\} \quad \text{for } (\bar{t}, \bar{x}) \in]0, \bar{T}[\times \bar{\Omega}_x \quad (4.16)$$

4.2. Effective problems

We are interested in the asymptotic behavior of the flow, thus of the models, for both short, intermediate and large times. For the asymptotic analysis, the question is related to the behavior of the dimensionless models above. More precisely, we want to describe the effective flow obtained for the short time $T = \bar{T}$, the intermediate time $T = \varepsilon^{-1} \bar{T}$ and the long time scales $T = \varepsilon^{-2} \bar{T}$.

Asymptotic expansion. We introduce the following formal asymptotics for the pressure and the velocity:

$$\bar{P}_\varepsilon^\gamma = \bar{P}_0^\gamma + \varepsilon \bar{P}_1^\gamma + \varepsilon^2 \bar{P}_2^\gamma + \dots \quad \bar{v}_\varepsilon^\gamma = \bar{v}_0^\gamma + \varepsilon \bar{v}_1^\gamma + \varepsilon^2 \bar{v}_2^\gamma + \dots \quad (4.17)$$

We emphasize that no arbitrary scaling is imposed, in particular we do not suppose as in [7] that the vertical velocity is much smaller than the horizontal one when the ratio ε is very small. We assume also the existence of formal asymptotics for the auxiliary variables appearing in (3.5)–(3.9)

$$\begin{cases} \bar{u}_\varepsilon^\gamma = \bar{u}_0^\gamma + \varepsilon \bar{u}_1^\gamma + \varepsilon^2 \bar{u}_2^\gamma + \dots & \bar{w}_\varepsilon^\gamma = \bar{w}_0^\gamma + \varepsilon \bar{w}_1^\gamma + \varepsilon^2 \bar{w}_2^\gamma + \dots \\ \bar{H}_\varepsilon^\gamma = \bar{H}_0 + \varepsilon \bar{H}_1^\gamma + \varepsilon^2 \bar{H}_2^\gamma + \dots & \bar{h}_\varepsilon^\gamma = \bar{h}_0 + \varepsilon \bar{h}_1^\gamma + \varepsilon^2 \bar{h}_2^\gamma + \dots, \end{cases} \quad (4.18)$$

and for the flux at the soil level

$$\bar{F}_\varepsilon = \bar{F}_0 + \varepsilon \bar{F}_1 + \varepsilon^2 \bar{F}_2 + \dots \quad (4.19)$$

Moreover, since s and k_r are \mathcal{C}^∞ by part functions, we write

$$\begin{cases} s(\bar{P}_\varepsilon^\gamma) = s(\bar{P}_0^\gamma) + \varepsilon(\bar{P}_1^\gamma + \varepsilon \bar{P}_2^\gamma + \dots) s'(\bar{P}_0^\gamma) + \frac{\varepsilon^2}{2} (\bar{P}_1^\gamma + \varepsilon \bar{P}_2^\gamma + \dots)^2 s''(\bar{P}_0^\gamma) + \dots \\ k_r(\bar{P}_\varepsilon^\gamma) = k_r(\bar{P}_0^\gamma) + \varepsilon(\bar{P}_1^\gamma + \varepsilon \bar{P}_2^\gamma + \dots) k_r'(\bar{P}_0^\gamma) + \frac{\varepsilon^2}{2} (\bar{P}_1^\gamma + \varepsilon \bar{P}_2^\gamma + \dots)^2 k_r''(\bar{P}_0^\gamma) + \dots \end{cases} \quad (4.20)$$

Effective problems at the main order. Let us introduce the following effective problems:

- related to the short time scale ($T = \bar{T}$),

$$\begin{cases} \phi \frac{\partial s(\bar{P}_0)}{\partial t} + \frac{\partial \bar{v}_0 \cdot e_3}{\partial \bar{z}} = 0 & \text{in }]0, \bar{T}[\times \Omega \\ \bar{v}_0 = -k_r(\bar{P}_0) \left(\frac{1}{\rho g} \frac{\partial \bar{P}_0}{\partial \bar{z}} + 1 \right) \bar{K}_0 e_3 & \text{in }]0, \bar{T}[\times \Omega \\ \alpha \bar{P}_0 + \beta \bar{v}_0 \cdot e_3 = \bar{F}_0 & \text{on }]0, \bar{T}[\times \bar{\Gamma}_{\text{soil}} \\ \bar{v}_0 \cdot e_3 = 0 & \text{on }]0, \bar{T}[\times \bar{\Gamma}_{\text{bot}} \end{cases} \quad (4.21)$$

- related to the non-short cases ($T = \varepsilon^{-1} \bar{T}$ or $T = \varepsilon^{-2} \bar{T}$),

$$\begin{cases} \bar{P}_0(t, x, z) = \rho g (\bar{H}_0(t, x) - \bar{z}) & \text{in }]0, \bar{T}[\times \bar{\Omega} \\ \bar{v}_0 = 0 & \text{in }]0, \bar{T}[\times \bar{\Omega} \end{cases} \quad (4.22)$$

- related to the non-short cases ($T = \varepsilon^{-1} \bar{T}$ or $T = \varepsilon^{-2} \bar{T}$) if $\alpha \neq 0$

$$\bar{H}_0(\bar{t}, \bar{x}) = \frac{\bar{F}_0(\bar{t}, \bar{x})}{\alpha \rho g} + \bar{h}_{\text{soil}}(\bar{t}, \bar{x}) \quad \text{in }]0, \bar{T}[\times \bar{\Omega}_x \quad (4.23)$$

- related to the intermediate time scale ($T = \varepsilon^{-1} \bar{T}$) if $\alpha = 0$ (and then $\beta \neq 0$)

$$\rho g \left(\int_{\bar{h}_{\text{bot}}}^{\bar{h}_{\text{soil}}} \phi s'(\bar{P}_0) dz \right) \frac{\partial \bar{H}_0}{\partial t} = -\frac{\bar{F}_1}{\beta} \quad \text{in }]0, \bar{T}[\times \bar{\Omega}_x \quad (4.24)$$

- related to the long time scale ($T = \varepsilon^{-2} \bar{T}$) if $\alpha = 0$

$$\begin{cases} -\text{div}_x (\bar{K}(\bar{H}_0) \nabla_x \bar{H}_0) = -\frac{\bar{F}_2}{\beta} - \frac{\partial}{\partial \bar{t}} \left(\int_{\bar{h}_{\text{bot}}}^{\bar{h}_{\text{soil}}} \phi s(\bar{P}_0) dz \right) & \text{in }]0, \bar{T}[\times \bar{\Omega}_x \\ \bar{K}(\bar{H}_0) \nabla_x \bar{H}_0 \cdot \bar{n} = 0 & \text{on }]0, \bar{T}[\times \bar{\Gamma}_{\text{ver}} \end{cases} \quad (4.25)$$

and concerning the first order of the velocity

$$\bar{v}_1 = -\bar{k}_r(\bar{P}_0) \bar{M}_0 \nabla_x \bar{H}_0 \quad \text{in }]0, \bar{T}[\times \bar{\Omega} \quad (4.26)$$

Proposition 4.1. Let $(\bar{P}_\varepsilon^\gamma, \bar{v}_\varepsilon^\gamma)$ be the solution of the rescaled 3D-Richards problem (4.9)–(4.10) or of the rescaled coupled model (4.12)–(4.16) for $T = \varepsilon^{-\gamma} \bar{T}$ and $\gamma \in \{0, 1, 2\}$. Assume that (4.17)–(4.20) hold true, then

- $(\bar{P}_0^0, \bar{v}_0^0)$ satisfies (4.21).
- $(\bar{P}_0^1, \bar{v}_0^1)$ satisfies (4.22) and (4.23) if $\alpha \neq 0$, or (4.22) and (4.24) with the compatibility condition $\bar{F}_0 = 0$ if $\alpha = 0$.
- $(\bar{P}_0^2, \bar{v}_0^2)$ satisfies (4.22) and (4.23) if $\alpha \neq 0$, or (4.22) and (4.25) with the compatibility condition $\bar{F}_0 = \bar{F}_1 = 0$ if $\alpha = 0$. Moreover \bar{v}_1^2 satisfies (4.26) if $\alpha = 0$.

We emphasize that the intermediate variable \bar{h} which characterizes the coupled model (4.11)–(4.15) does not appear in any of the main order effective problems (4.21)–(4.25). This agrees with the fact that the whole class of models given by (3.5)–(3.9) for any h satisfying (3.5) can approximate the reference Richards model.

4.3. Proof of Proposition 4.1 for the Richards model

The proof of Proposition 4.1 consists in substituting the formal asymptotic expansion (4.17)–(4.20) in the rescaled 3D-Richards problem (4.9)–(4.10). A cascade of equations follows by identifying the powers of ε . Then we characterize the main order terms in the expansion (4.17). In order to reduce ratings in this section, we do not write the exponent γ on the variables name.

General relations. Let us start by obtaining the first relations holding in every time scale (i.e. for all $\gamma \in \{0, 1, 2\}$). By plugging the asymptotic expansion (4.17) in the first equation of (4.10) we get the following relations holding in $]0, \bar{T}[\times \bar{\Omega}$

$$\begin{cases} \bar{v}_0 = -k_r(\bar{P}_0) \left(\frac{1}{\rho g} \frac{\partial \bar{P}_0}{\partial \bar{z}} + 1 \right) \bar{K}_0 e_3, \\ \bar{v}_1 = -\frac{k_r(\bar{P}_0)}{\rho g} \bar{K}_0 \left(\nabla_{\bar{x}} \bar{P}_0 + \frac{\partial \bar{P}_1}{\partial \bar{z}} e_3 \right) - k'_r(\bar{P}_0) \bar{P}_1 \left(\frac{1}{\rho g} \frac{\partial \bar{P}_0}{\partial \bar{z}} + 1 \right) \bar{K}_0 e_3. \end{cases} \quad (4.27)$$

The same process in the three last equations of (4.10) yields the following relations in $]0, \bar{T}[$:

- on $\bar{\Gamma}_{\text{soil}}$

$$\begin{cases} \alpha \bar{P}_0 + \beta \bar{v}_0 \cdot e_3 = \bar{F}_0, & \alpha \bar{P}_1 + \beta (\bar{v}_1 \cdot e_3 - \bar{v}_0 \cdot \nabla_{\bar{x}} \bar{h}_{\text{soil}}) = \bar{F}_1, \\ \alpha \left(\bar{P}_2 + \frac{1}{2} \|\nabla_{\bar{x}} \bar{h}_{\text{soil}}\|^2 \bar{P}_0 \right) + \beta (\bar{v}_2 \cdot e_3 - \bar{v}_1 \cdot \nabla_{\bar{x}} \bar{h}_{\text{soil}}) = \frac{1}{2} \|\nabla_{\bar{x}} \bar{h}_{\text{soil}}\|^2 \bar{F}_0 + \bar{F}_2; \end{cases} \quad (4.28)$$

- on $\bar{\Gamma}_{\text{bot}}$, for all $k \in \mathbb{N}^*$

$$\bar{v}_0 \cdot e_3 = 0, \quad \bar{v}_{k-1} \cdot \nabla_{\bar{x}} \bar{h}_{\text{bot}} = \bar{v}_k \cdot e_3; \quad (4.29)$$

- on $\bar{\Gamma}_{\text{ver}}$, for all $k \in \mathbb{N}$

$$\bar{v}_k \cdot \bar{n} = 0. \quad (4.30)$$

Short time case. We prove the first claim of Proposition 4.1 which is associated with the short characteristic time scale $T = \varepsilon^{-\gamma} \bar{T}$ for $\gamma = 0$. The equation (4.9) here reads

$$\phi \frac{\partial s(\bar{P})}{\partial \bar{t}} + \varepsilon \operatorname{div}_{\bar{x}}(\bar{v}) + \frac{\partial \bar{v} \cdot e_3}{\partial \bar{z}} = 0. \quad (4.31)$$

Some computations show that the main order terms in the latter equation give

$$\phi \frac{\partial s(\bar{P}_0)}{\partial \bar{t}} + \frac{\partial \bar{v}_0 \cdot e_3}{\partial \bar{z}} = 0 \quad \text{in }]0, \bar{T}[\times \bar{\Omega}. \quad (4.32)$$

The latter equation completed with the first equations of (4.27), (4.28) and (4.29) gives exactly the system (4.21). The first claim of Proposition 4.1 is proven.

Intermediate time case. In this part, we prove the second claim of Proposition 4.1 which is associated with the intermediate time scale $T = \varepsilon^{-\gamma} \bar{T}$ for $\gamma = 1$. Equation of (4.9) is now

$$\varepsilon \phi \frac{\partial s(\bar{P})}{\partial \bar{t}} + \varepsilon \operatorname{div}_{\bar{x}}(\bar{v}) + \frac{\partial \bar{v} \cdot e_3}{\partial \bar{z}} = 0. \quad (4.33)$$

We introduce the asymptotic expansion (4.17) in the previous equation and we identify the main order terms. We obtain

$$\frac{\partial \bar{v}_0 \cdot e_3}{\partial \bar{z}} = 0 \quad \text{on }]0, \bar{T}[\times \bar{\Omega}. \quad (4.34)$$

This constant vertical velocity is actually zero due to (4.29). Moreover, with the first equation of (4.27) and since k_r and $(\bar{K}_0)_{33}$ are non-vanishing (\bar{K}_0 is positive definite), we get in $]0, \bar{T}[\times \bar{\Omega}$

$$\frac{\partial \bar{P}_0}{\partial \bar{z}} + \rho g = 0 \quad \text{and} \quad \bar{v}_0 = 0. \quad (4.35)$$

The existence of $\bar{H}_0 = \bar{H}_0(t, x)$ such that

$$\bar{P}_0(t, x, z) = \rho g(\bar{H}_0(t, x) - \bar{z}) \quad \text{in }]0, \bar{T}[\times \bar{\Omega} \quad (4.36)$$

follows. Next, since $\bar{v}_0 = 0$, the first equation of (4.28) is

$$\alpha \bar{P}_0 = \bar{F}_0 \quad \text{on } \bar{\Gamma}_{\text{soil}}. \quad (4.37)$$

We now have to differentiate the computations depending on whether $\alpha = 0$ or not.

If $\alpha \neq 0$, then for all $(\bar{t}, \bar{x}) \in]0, \bar{T}[\times \bar{\Omega}_x$ we have $\bar{P}_0(\bar{t}, \bar{x}, \bar{h}_{\text{soil}}(\bar{t}, \bar{x})) = \bar{F}_0(\bar{t}, \bar{x})/\alpha$. Accordingly, thanks to (4.36), it holds

$$\bar{H}_0(\bar{t}, \bar{x}) = \frac{\bar{F}_0(\bar{t}, \bar{x})}{\alpha \rho g} + \bar{h}_{\text{soil}}(\bar{t}, \bar{x}).$$

This ends the proof of the second claim of Proposition 4.1 in the case $\alpha \neq 0$.

If $\alpha = 0$ (then $\beta \neq 0$), equation (4.37) only implies that $\bar{F}_0 = 0$. In particular, \bar{H}_0 remains as a degree of freedom and we have to exploit the next order terms in the asymptotic expansion for the closure of the effective problem. Identifying the coefficients associated with ε^1 in equation (4.33) we have

$$\phi \frac{\partial s(\bar{P}_0)}{\partial \bar{t}} + \frac{\partial \bar{v}_1 \cdot e_3}{\partial \bar{z}} = 0 \quad \text{in }]0, \bar{T}[\times \bar{\Omega}. \quad (4.38)$$

To eliminate \bar{v}_1 , we integrate vertically on $] \bar{h}_{\text{bot}}, \bar{h}_{\text{soil}}[$ the equation above. After using the fact that $\partial_t(s(\bar{P}_0)) = \rho g s'(\bar{P}_0) \partial_t \bar{H}_0$ (consequence of (4.36)) we have

$$\rho g \left(\int_{\bar{h}_{\text{bot}}}^{\bar{h}_{\text{soil}}} \phi s'(\bar{P}_0) dz \right) \frac{\partial \bar{H}_0}{\partial t} + (\bar{v}_1|_{\bar{h}_{\text{soil}}} - \bar{v}_1|_{\bar{h}_{\text{bot}}}) \cdot e_3 = 0. \quad (4.39)$$

Thanks to the second equations of (4.28) and (4.29) in the case where $\alpha = 0$ and $\bar{v}_0 = 0$, it follows:

$$\bar{v}_1 \cdot e_3 = \bar{F}_1 / \beta \quad \text{on } \bar{\Gamma}_{\text{soil}} \quad \text{and} \quad \bar{v}_1 \cdot e_3 = 0 \quad \text{on } \bar{\Gamma}_{\text{bot}}.$$

Accordingly, equation (4.39) becomes

$$\rho g \left(\int_{\bar{h}_{\text{bot}}}^{\bar{h}_{\text{soil}}} \phi s'(\bar{P}_0) dz \right) \frac{\partial \bar{H}_0}{\partial t} = -\frac{\bar{F}_1}{\beta}. \quad (4.40)$$

Finally, collecting equations (4.36) and (4.40) we get $\bar{v}_0 = 0$ and

$$\begin{cases} \bar{P}_0(\bar{t}, \bar{x}, \bar{z}) = \rho g(\bar{H}_0(\bar{t}, \bar{x}) - \bar{z}) & \text{in }]0, \bar{T}[\times \bar{\Omega} \\ \rho g \left(\int_{\bar{h}_{\text{bot}}}^{\bar{h}_{\text{soil}}} \phi s'(\bar{P}_0) dz \right) \frac{\partial \bar{H}_0}{\partial t} = -\frac{\bar{F}_1}{\beta} & \text{in }]0, \bar{T}[\times \bar{\Omega}_x \end{cases} \quad (4.41)$$

which correspond to the second claim of Proposition 4.1 in the case $\alpha = 0$.

Long time case. In this part, we prove the third claim of Proposition 4.1 which is associated with the intermediate time scale $T = \varepsilon^{-\gamma} \bar{T}$ for $\gamma = 2$. Equation (4.9) takes the form

$$\varepsilon^2 \phi \frac{\partial s(\bar{P})}{\partial \bar{t}} + \varepsilon \operatorname{div}_{\bar{x}}(\bar{v}) + \frac{\partial \bar{v} \cdot e_3}{\partial \bar{z}} = 0. \quad (4.42)$$

We substitute the asymptotic expansion (4.17) in the previous equation. The main order part of the equation is $\partial_z(\bar{v}_0 \cdot e_3) = 0$ which leads, as before, to (4.22) for some function \bar{H}_0 which does not depend on \bar{z} . The same relation (4.37) holds and the characterization of \bar{H}_0 depends on the values of α . As before, if $\alpha \neq 0$ we have (4.23).

It remains to deal with the case $\alpha = 0$ and to exhibit the equations of system (4.25). In this case, the compatibility condition $F_0 = 0$ holds as before because of (4.37). The characterization of \bar{H}_0 needs to go at the next order in the asymptotic expansion. In equation (4.42) we get

$$0 = \operatorname{div}_{\bar{x}}(\bar{v}_0) + \frac{\partial \bar{v}_1 \cdot e_3}{\partial \bar{z}} = \frac{\partial \bar{v}_1 \cdot e_3}{\partial \bar{z}} \quad (4.43)$$

where the second equality is due to $\bar{v}_0 = 0$. Moreover, the second equations of (4.28) and (4.29) for $k = 1$ lead to (since $\alpha = 0$)

$$\beta \bar{v}_1 \cdot e_3 = \bar{F}_1 \quad \text{on } \bar{\Gamma}_{\text{soil}} \quad \text{and} \quad \bar{v}_1 \cdot e_3 = 0 \quad \text{on } \bar{\Gamma}_{\text{bot}}. \quad (4.44)$$

Then, the vertical component of the velocity (which is constant by (4.43)) $\bar{v}_1 \cdot e_3$ is zero. Moreover the second compatibility condition $\bar{F}_1 = 0$ holds true thanks to (4.44). Using the second equation of (4.27) and bearing in mind that $(\rho g)^{-1} \partial_z \bar{P}_0 + 1 = 0$, we obtain

$$\bar{v}_1 = -\frac{k_r(\bar{P}_0)}{\rho g} \bar{K}_0 \left(\nabla_{\bar{x}} \bar{P}_0 + \frac{\partial \bar{P}_1}{\partial \bar{z}} e_3 \right). \quad (4.45)$$

Since $\bar{v}_1 \cdot e_3 = 0$, using the same notation for \bar{K}_0 than in (2.6), we compute $\partial_z \bar{P}_1$ by

$$\frac{\partial \bar{P}_1}{\partial \bar{z}} = -\frac{1}{\bar{K}_{zz}} \bar{K}_0 \nabla_{\bar{x}} \bar{P}_0 \cdot e_3.$$

Finally, substitution in the equation above with the relation $\bar{P}_0 = \rho g(\bar{H}_0 - z)$ give

$$\bar{v}_1 = -k_r(\bar{P}_0) \bar{M}_0 \nabla_{\bar{x}} \bar{H}_0 \quad \text{with} \quad \bar{M}_0 = \begin{pmatrix} I_2 & -\frac{\bar{K}_{xz}}{\bar{K}_{zz}} \\ 0 & 0 \end{pmatrix} \bar{K}_0 = \begin{pmatrix} \bar{S}_0 & 0 \\ 0 & 0 \end{pmatrix} \quad (4.46)$$

where I_2 is the $2d$ identity matrix and $\bar{S}_0 = \bar{K}_{xx} - \bar{K}_{zz}^{-1} \bar{K}_{xz} \bar{K}_{zx}$.

On the other hand, the equation (4.30) for $k = 1$ leads to $\bar{v}_1 \cdot \bar{n} = 0$ on $\bar{\Gamma}_{\text{ver}}$. Since $k_r(\bar{P}_0)$ does not vanish, we obtain the last equation of (4.25). After identifying the coefficients associated with ε^2 in equation (4.42) we get

$$\phi \frac{\partial s(\bar{P}_0)}{\partial \bar{t}} + \operatorname{div}_{\bar{x}}(\bar{v}_1) + \frac{\partial \bar{v}_2 \cdot e_3}{\partial \bar{z}} = 0. \quad (4.47)$$

Taking into account (4.22), (4.46) and the fact that $\alpha = F_0 = 0$, the third equation of (4.28) and the second equations of (4.29) for $k = 2$ become

$$\bar{v}_2 \cdot e_3 - \bar{v}_1 \cdot \nabla_{\bar{x}} \bar{h}_{\text{soil}} = \bar{F}_2 / \beta, \quad \bar{v}_2 \cdot e_3 - \bar{v}_1 \cdot \nabla_{\bar{x}} \bar{h}_{\text{bot}} = 0 \quad \text{on } \bar{\Gamma}_{\text{bot}}. \quad (4.48)$$

To eliminate v_2 in system (4.47)–(4.48), we integrate (4.47) with respect to \bar{z} on $[\bar{h}_{\text{bot}}, \bar{h}_{\text{soil}}]$. Taking into account the boundary conditions on $\bar{\Gamma}_{\text{bot}}$ and $\bar{\Gamma}_{\text{soil}}$ we obtain

$$\frac{\partial}{\partial \bar{t}} \int_{\bar{h}_{\text{bot}}}^{\bar{h}_{\text{soil}}} \phi s(\bar{P}_0) d\bar{z} + \int_{\bar{h}_{\text{bot}}}^{\bar{h}_{\text{soil}}} \operatorname{div}_{\bar{x}} \bar{v}_1 d\bar{z} + \bar{v}_1|_{\bar{h}_{\text{soil}}} \cdot \nabla_{\bar{x}} \bar{h}_{\text{soil}} + \frac{\bar{F}_2}{\beta} - \bar{v}_1|_{\bar{h}_{\text{bot}}} \cdot \nabla_{\bar{x}} \bar{h}_{\text{bot}} = 0.$$

We use the Leibniz rule in the second integral and we get

$$\frac{\partial}{\partial \bar{t}} \int_{\bar{h}_{\text{bot}}}^{\bar{h}_{\text{soil}}} \phi s(\bar{P}_0) d\bar{z} + \operatorname{div}_{\bar{x}} \left(\int_{\bar{h}_{\text{bot}}}^{\bar{h}_{\text{soil}}} \bar{v}_1 d\bar{z} \right) = -\frac{\bar{F}_2}{\beta}. \quad (4.49)$$

Using the averaged conductivity \bar{K} defined in (4.3), we get, with the first equation of (4.46),

$$\int_{\bar{h}_{\text{bot}}}^{\bar{h}_{\text{soil}}} \bar{v}_1 d\bar{z} = -\int_{\bar{h}_{\text{bot}}}^{\bar{h}_{\text{soil}}} k_r(\bar{P}_0) \bar{M}_0 \nabla_{\bar{x}} \bar{H}_0 = -\bar{K}(\bar{H}_0) \nabla_{\bar{x}} \bar{H}_0.$$

The above equation associated with equation (4.49) is exactly the system (4.25). This ends the proof of the last claim of Proposition (4.1).

4.4. Proof of Proposition 4.1 for the coupled models

The strategy of the proof is exactly the same than in the previous subsection.

General relations. Let $\gamma \in \{0, 1, 2\}$. Using the expansion (4.17)–(4.20), we identify powers of ε in all the equations in (4.11)–(4.16) that does not depend on the time scale T . We obtain from the second equation of (4.11)

$$\begin{cases} \bar{u}_0 = -k_r(\bar{P}_0) \left(\frac{1}{\rho g} \frac{\partial \bar{P}_0}{\partial \bar{z}} + 1 \right) \bar{K}_0 e_3 & \text{in }]0, \bar{T}[\times \bar{\Omega}, \\ \bar{u}_1 = -\frac{k_r(\bar{P}_0)}{\rho g} \frac{\partial \bar{P}_1}{\partial \bar{z}} \bar{K}_0 e_3 - k'_r(\bar{P}_0) \bar{P}_1 \left(\frac{1}{\rho g} \frac{\partial \bar{P}_0}{\partial \bar{z}} + 1 \right) \bar{K}_0 e_3 & \text{in }]0, \bar{T}[\times \bar{\Omega}, \end{cases} \quad (4.50)$$

from the third equation of (4.11)

$$\bar{w}_0 = 0, \quad \bar{w}_1 = -k_r(\rho g(\bar{H}_0 - \bar{z})) \bar{M}_0 \nabla_{\bar{x}} \bar{H}_0 \quad \text{in }]0, \bar{T}[\times \bar{\Omega}, \quad (4.51)$$

from the first equation of (4.11)

$$\begin{cases} \bar{v}_0 = \bar{u}_0 + \bar{w}_0 = \bar{u}_0 = -k_r(\bar{P}_0) \left(\frac{1}{\rho g} \frac{\partial \bar{P}_0}{\partial \bar{z}} + 1 \right) \bar{K}_0 e_3 & \text{in }]0, \bar{T}[\times \bar{\Omega}, \\ \bar{v}_1 = \bar{u}_1 + \bar{w}_1 & \text{in }]0, \bar{T}[\times \bar{\Omega}. \end{cases} \quad (4.52)$$

It follows from (4.13) that for $\bar{t} \in]0, \bar{T}[$ and $(\bar{x}, \bar{z}) \in \Omega_{h_0}^-(\bar{t})$

$$\bar{P}_0(\bar{t}, \bar{x}, \bar{z}) = \rho g(\bar{H}_0(\bar{t}, \bar{x}) - \bar{z}), \quad \bar{P}_k(\bar{t}, \bar{x}, \bar{z}) = \rho g \bar{H}_k(\bar{t}, \bar{x}) \quad \forall k > 0. \quad (4.53)$$

Equation (4.16) gives

$$\bar{h}_{\text{bot}}(\bar{x}) \leq \bar{h}_0(\bar{t}, \bar{x}) \leq \max \left\{ \min \left\{ \bar{H}_0(\bar{t}, \bar{x}) - \frac{\bar{P}_s}{\rho g}, \bar{h}_{\text{max}}(\bar{x}) \right\}, \bar{h}_{\text{bot}}(\bar{x}) \right\} \quad \text{in }]0, \bar{T}[\times \bar{\Omega}_x. \quad (4.54)$$

For the boundary conditions, we infer from the second and third equations of (4.12) and from the second equation of (4.14) that, for all $k \in \mathbb{N}$,

$$\begin{cases} \alpha \bar{P}_k + \beta \bar{u}_k \cdot e_3 = \bar{F}_k & \text{on }]0, \bar{T}[\times \bar{\Gamma}_{\text{soil}}, \\ \bar{P}_0(\bar{t}, \bar{x}, \bar{h}_0(\bar{t}, \bar{x})) = \rho g(\bar{H}_0(\bar{t}, \bar{x}) - \bar{h}_0(\bar{t}, \bar{x})) & \text{for } \bar{t} \in]0, \bar{T}[, \quad \bar{x} \in \Gamma_{\bar{h}}(\bar{t}), \\ \bar{K}(\bar{H}_0) \nabla_{\bar{x}} \bar{H}_0 \cdot \bar{n} = 0 & \text{on }]0, \bar{T}[\times \bar{\Gamma}_{\text{ver}}. \end{cases} \quad (4.55)$$

By (4.53) for $k = 1$, $\partial_z \bar{P}_1 = 0$ on $\Omega_{h_0}^-(\bar{t})$. Then by (4.50) and the first equation of (4.53)

$$\bar{u}_1 = 0 \quad \text{in } \Omega_{h_0}^-(\bar{t}). \quad (4.56)$$

Short time case. In this part, $T = \bar{T}$, that is $\gamma = 0$. The first equations of (4.12) and (4.14) become

$$\begin{cases} \phi \frac{\partial s(\bar{P})}{\partial t} + \frac{\partial}{\partial \bar{z}} (\bar{u} \cdot e_3) = 0 & \text{for } \bar{t} \in]0, \bar{T}[, \quad (\bar{x}, \bar{z}) \in \Omega_{\bar{h}}^+(\bar{t}), \\ \varepsilon^2 \operatorname{div}_x (\bar{K}(\bar{H}) \nabla \bar{H}) = (\bar{u}_0 \cdot e_3)|_{\Gamma_{\bar{h}}} & \text{for } (\bar{t}, \bar{x}) \in]0, \bar{T}[\times \bar{\Omega}_x. \end{cases} \quad (4.57)$$

We identify the main order terms appearing when the asymptotics (4.17)–(4.20) are substituted in the previous equations: for $\bar{t} \in]0, \bar{T}[$ and $(\bar{x}, \bar{z}) \in \Omega_{h_0}^+(\bar{t})$

$$\phi \frac{\partial s(\bar{P}_0)}{\partial t} + \frac{\partial}{\partial \bar{z}} (\bar{u}_0 \cdot e_3) = 0, \quad (4.58)$$

$$(\bar{u}_0 \cdot e_3)|_{\Gamma_{\bar{h}_0}} = 0 \quad \text{for } (\bar{t}, \bar{x}) \in]0, \bar{T}[\times \bar{\Omega}_x. \quad (4.59)$$

From (4.52) and (4.53) we also compute $\bar{u}_0 = 0$ in $\Omega_{\bar{h}_0}^-(\bar{t})$. In addition, from (4.54) we get $s(\bar{P}_0) = 1$ in $\Omega_{\bar{h}}^-(\bar{t})$ so that (\bar{P}_0, \bar{u}_0) satisfies (4.58) also in $\Omega_{\bar{h}}^-(\bar{t})$. The continuity of $\bar{u}_0 \cdot e_3$ being ensured by (4.59), (\bar{P}_0, \bar{u}_0) satisfies (4.58) in the whole Ω . By using (4.52) and (4.55) we obtain the system (4.21) and then the first claim of Proposition 4.1 holds once again.

Intermediate time case. In this part, $T = \varepsilon^{-1}\bar{T}$, $\gamma = 1$. The first equation of (4.12) and the equation (4.15) become

$$\begin{cases} \phi \varepsilon \frac{\partial s(\bar{P})}{\partial t} + \frac{\partial}{\partial z}(\bar{u} \cdot e_3) = 0 & \text{for } \bar{t} \in]0, \bar{T}[, \quad (\bar{x}, \bar{z}) \in \Omega_{\bar{h}}^{\pm}(\bar{t}) \\ -\varepsilon^2 \operatorname{div}_x(\bar{K}(\bar{H}) \nabla_x \bar{H}) = -(\bar{u} \cdot e_3)|_{\bar{\Gamma}_{\text{soil}}} - \varepsilon \frac{\partial}{\partial t} \left(\int_{\bar{h}_{\text{bot}}(t,x)}^{\bar{h}_{\text{soil}}(x)} \phi s(\bar{P}) dz \right) & \text{for } (\bar{t}, \bar{x}) \in]0, \bar{T}[\times \bar{\Omega}_x \end{cases} \quad (4.60)$$

The corresponding main order relations are

$$\bar{u}_0 \cdot e_3 = 0 \quad \text{on }]0, \bar{T}[\times \bar{\Gamma}_{\text{soil}} \quad (4.61)$$

and for $\bar{t} \in]0, \bar{T}[$ and $(\bar{x}, \bar{z}) \in \Omega_{\bar{h}}^{\pm}(\bar{t})$,

$$\frac{\partial}{\partial z}(\bar{u}_0 \cdot e_3) = 0. \quad (4.62)$$

It follows that the constant vertical component of the velocity $\bar{u}_0 \cdot e_3$ equals zero in $\Omega_{\bar{h}}^{\pm}(\bar{t})$. We deduce from the first equation of (4.50) that the pressure \bar{P}_0 is affine with respect to the z variable with the slope $-\rho g$ in $\Omega_{\bar{h}}^{\pm}(\bar{t})$. Accordingly, thanks to the first equation of (4.53) and the continuity condition given in (4.55), the first equation of (4.22) holds. Using relation (4.52) we obtain the second equation of (4.22). Next, thanks to $\bar{u}_0 = 0$ and to the first equation of (4.55) for $k = 0$, we get $\alpha P_0 = \bar{F}_0$.

If $\alpha \neq 0$ then for all $(t, x) \in]0, T[\times \Omega_x$ we have $P_0(\bar{t}, \bar{x}, \bar{h}_{\text{soil}}(\bar{t}, \bar{x})) = \bar{F}_0(\bar{t}, \bar{x})/\alpha$. Accordingly, thanks to the first equation of (4.22), we have

$$\bar{H}_0(\bar{t}, \bar{x}) = \frac{\bar{F}_0(\bar{t}, \bar{x})}{\alpha \rho g} + \bar{h}_{\text{soil}}(\bar{t}, \bar{x}).$$

The second claim of Proposition 4.1 in the case $\alpha \neq 0$ is proved.

If $\alpha = 0$, the compatibility condition $\bar{F}_0 = 0$ is imposed. After identifying the coefficients associated with ε^1 in the second equation of (4.60) we have

$$0 = -(\bar{u}_1 \cdot e_3)|_{\bar{\Gamma}_{\text{soil}}} - \frac{\partial}{\partial t} \left(\int_{\bar{h}_{\text{bot}}(x)}^{\bar{h}_{\text{soil}}(x)} \phi s(\bar{P}_0) dz \right)$$

and, with the first equation of (4.22),

$$\rho g \left(\int_{\bar{h}_{\text{bot}}(x)}^{\bar{h}_{\text{soil}}(x)} \phi s'(\bar{P}_0) dz \right) \frac{\partial \bar{H}_0}{\partial t} = -(\bar{u}_1 \cdot e_3)|_{\bar{\Gamma}_{\text{soil}}}.$$

The first equation of (4.55) for $k = 1$ implies, since $\alpha = 0$, that $(\bar{u}_1 \cdot e_3)|_{\bar{\Gamma}_{\text{soil}}} = \bar{F}_1/\beta$. This ends the proof of the second claim of Proposition 4.1 in the case $\alpha = 0$.

Long time case. In this part, $T = \varepsilon^{-\gamma}\bar{T}$, $\gamma = 2$. The first equation of (4.12) and equation (4.15) are now

$$\begin{cases} \phi \varepsilon^2 \frac{\partial s(\bar{P})}{\partial t} + \frac{\partial}{\partial z}(\bar{u} \cdot e_3) = 0 & \text{for } \bar{t} \in]0, \bar{T}[, \quad (\bar{x}, \bar{z}) \in \Omega_{\bar{h}}^{\pm}(\bar{t}) \\ -\varepsilon^2 \operatorname{div}_{\bar{x}}(\bar{K}(\bar{H}) \nabla_{\bar{x}} \bar{H}) = -(\bar{u} \cdot e_3)|_{\bar{\Gamma}_{\text{soil}}} - \varepsilon^2 \frac{\partial}{\partial t} \left(\int_{\bar{h}_{\text{bot}}(\bar{x})}^{\bar{h}_{\text{soil}}(\bar{x})} \phi s(\bar{P}) dz \right) & \text{for } (\bar{t}, \bar{x}) \in]0, \bar{T}[\times \bar{\Omega}_x \end{cases} \quad (4.63)$$

As in the intermediate time case, we substitute asymptotics (4.17)–(4.20) in the previous equations. Identifying the coefficients associated with ε^n for $n \in \{1, 2\}$, we get $\partial_z(\bar{u}_n \cdot e_3) = 0$ in $\Omega_h^\pm(\bar{t})$ and $\bar{u}_n \cdot e_3 = 0$ on $\bar{\Gamma}_{\text{soil}}$. This leads to

$$\bar{u}_0 \cdot e_3 = \bar{u}_1 \cdot e_3 = 0 \quad \text{on } \Omega_h^\pm(\bar{t}). \quad (4.64)$$

By using the same arguments we obtain $\bar{P}_0 = \rho g(\bar{H}_0 - z)$ and $\bar{v}_0 = 0$ in whole Ω . System (4.22) is satisfied. The characterization of \bar{H}_0 depends on the values of α . Similar arguments to those employed in the intermediate time case when $\alpha \neq 0$ lead to (4.23).

It remains to deal with the case $\alpha = 0$. In this case we first remark that the compatibility condition $\bar{F}_0 = 0$ holds (see (4.55) for $k = 0$). Furthermore, since $\bar{P}_0 = \rho g(\bar{H}_0 + z)$ we get from (4.56) and (4.64) that $\bar{u}_1 = 0$ in $]0, \bar{T}[\times \bar{\Omega}$. Thus, using (4.51) and (4.52) we get $\bar{v}_1 = \bar{w}_1 = -k_r(\bar{P}_0)\bar{M}_0 \nabla_x \bar{H}_0$. Moreover the first equation of (4.55) for $k = 1$ gives $\bar{F}_1 = 0$ (since $\alpha = 0$). It remains to get the first relation of system (4.25). By plugging asymptotics (4.17)–(4.20) in the second equation of (4.63) and by identifying the coefficients associated with ε^2 we get ((4.50))

$$-\operatorname{div}_x(\bar{K}(\bar{H}_0) \nabla_x \bar{H}_0) = -(\bar{u}_2 \cdot e_3)|_{\bar{\Gamma}_{\text{soil}}} - \frac{\partial}{\partial \bar{t}} \left(\int_{\bar{h}_{\text{bot}}(x)}^{\bar{h}_{\text{soil}}(x)} \phi s(\bar{P}_0) dz \right) \quad \text{for } (\bar{t}, \bar{x}) \in]0, \bar{T}[\times \bar{\Omega}_x. \quad (4.65)$$

We end the proof by noting that, thanks to the equality $\alpha = 0$ and the first equation of (4.55) for $k = 2$, we have $(\bar{u}_2 \cdot e_3)|_{\bar{\Gamma}_{\text{soil}}} = \bar{F}_2 / \beta$. \square

REFERENCES

- [1] MB Abbott, JC Bathurst, JA Cunge, PE O'connell, and J Rasmussen. An introduction to the european hydrological system - systeme hydrologique europeen, "she", 2: Structure of a physically-based, distributed modelling system. *Journal of Hydrology*, 87(1):61–77, 1986.
- [2] Christine Bernardi, Adel Blouza, and Linda El Alaoui. The rain on underground porous media part i: Analysis of a richards model. *Chinese Annals of Mathematics, Series B*, 34(2):193–212, Mar 2013.
- [3] Heiko Berninger, Mario Ohlberger, Oliver Sander, and Kathrin Smetana. Unsaturated subsurface flow with surface water and nonlinear in- and outflow conditions. *Mathematical Models and Methods in Applied Sciences*, 24(05):901–936, 2014.
- [4] R.H. Brooks and A.T. Corey. *Hydraulic Properties of Porous Media*. Colorado State University Hydrology Papers. Colorado State University, 1964.
- [5] Bear Jacob. *Dynamics of fluids in porous media*. Elsevier, New-York, 1972.
- [6] Bear Jacob and Verruijt Arnold. *Modeling groundwater flow and pollution*. Springer, Netherlands, 1987.
- [7] M. Jazar and R. Monneau. Derivation of seawater intrusion models by formal asymptotics. *SIAM J. Appl. Math.*, 74(4):1152–1173, 2014.
- [8] Jun Kong, Pei Xin, Zhi yao Song, and Ling Li. A new model for coupling surface and subsurface water flows: With an application to a lagoon. *Journal of Hydrology*, 390(1):116 – 120, 2010.
- [9] Gary Pantelis. Saturated-unsaturated flow in unconfined aquifers. *Zeitschrift für angewandte Mathematik und Physik ZAMP*, 36(5):648–657, Sep 1985.
- [10] Raphaël Paulus, Benjamin J. Dewals, Sébastien Erpicum, Michel Piroton, and Pierre Archambeau. Innovative modelling of 3d unsaturated flow in porous media by coupling independent models for vertical and lateral flows. *Journal of Computational and Applied Mathematics*, 246:38 – 51, 2013. Fifth International Conference on Advanced COmputational Methods in ENgineering (ACOMEN 2011).
- [11] Hung Q Pham, Delwyn G Fredlund, and S Lee Barbour. A study of hysteresis models for soil-water characteristic curves. *Canadian Geotechnical Journal*, 42(6):1548–1568, 2005.
- [12] Mary F Pikul, Robert L Street, and Irwin Remson. A numerical model based on coupled one-dimensional richards and boussinesq equations. *Water Resources Research*, 10(2):295–302, 1974.
- [13] Ben Schweizer. Hysteresis in porous media: Modelling and analysis. *Interfaces and Free Boundaries*, 19:417–447, 01 2017.
- [14] P. Sochala, A. Ern, and S. Piperno. Mass conservative bdf-discontinuous galerkin/explicit finite volume schemes for coupling subsurface and overland flows. *Computer Methods in Applied Mechanics and Engineering*, 198(27):2122 – 2136, 2009.
- [15] Georges Vachaud and Michel Vauclin. Comments on 'a numerical model based on coupled one-dimensional richards and boussinesq equations' by mary f. pikul, robert l. street, and irwin remson. *Water Resources Research*, 11(3):506–509, 1975.
- [16] M Th Van Genuchten. A closed-form equation for predicting the hydraulic conductivity of unsaturated soils 1. *Soil science society of America journal*, 44(5):892–898, 1980.
- [17] A. Yakirevich, V. Borisov, and S. Sorek. A quasi three-dimensional model for flow and transport in unsaturated and saturated zones: 1. implementation of the quasi two-dimensional case. *Advances in Water Resources*, 21(8):679 – 689, 1998.